

**A FINITE ELEMENT STUDY OF BENDING STRESS VARIATION IN MESHED SPUR
GEAR PAIRS**

by

Ming-Fa Feng

Thesis submitted to the Faculty of the
Virginia Polytechnic Institute and State University
in partial fulfillment of the requirements for the degree of
Master of Science
in
Mechanical Engineering

APPROVED:

R. G. Mitchiner, Chairman

H. H. Mabie

C. E. Knight

October, 1987

Blacksburg, Virginia

**A FINITE ELEMENT STUDY OF BENDING STRESS VARIATION IN MESHED SPUR
GEAR PAIRS**

by

Ming-Fa Feng

R. G. Mitchiner, Chairman

Mechanical Engineering

(ABSTRACT)

A study of the bending stresses in a pair of meshed spur gears using the finite element method is presented. The models analyzed were in the shape of a circular gear with five teeth or a five-tooth rack. A unit torque (1 lbf-ft) was applied as the form of nodal forces on the nodes around the bore hole of the driver pinion. The nodes around the bore hole of the driven gear (or the nodes along the back of the driven rack) were fixed. In order to transmit the power from the driver pinion to the driven gear (or rack), the points in contact were made coincident.

Seven model groups with same diametral pitch (1.0), addendum (1.0 in.), dedendum (1.3 in.), pressure angle (20°) and hob tip radius (0.35 in.) but with varying numbers of teeth on the pinion and gear were analyzed to compute the tensile stress variation in the root fillet during the duration of contact. A model for predicting the tensile stress variation at the root fillet during the duration of contact has been created.

The results were compared with AGMA and other results with agreement for the peak within 3%.

Acknowledgements

The author wishes to thank Dr. R. G. Mitchiner for his advice and guidance during the course of this study. Appreciation is also extended to Dr. C. E. Knight and Dr. H. H. Mabie for their service on the Graduate Committee and their advice and assistance.

Table of Contents

1.0	Introduction	1
2.0	Literature Review	5
3.0	Geometry Modeling of Meshed Spur Gear Pairs	7
3.1	Introduction	7
3.2	Using TOOTH [Appendix B] to generate meshed spur gear models	8
3.3	Duration of contact	13
3.4	Contact ratio	17
3.5	Model for a pinion meshing with a rack	20
3.6	SUPERTAB	22
3.7	SUPERB	22
4.0	Finite Element Modeling and Analysis	24
4.1	Modeling	24
4.2	Model size study	28
4.3	Load magnitude effects	32

4.4	Description of models	32
5.0	Results	37
6.0	Conclusions and Recommendations	63
	Bibliography	69
	Appendix A. Geometry of The Spur Tooth	71
A.1	Introduction	71
A.2	Tooth profile definition	71
A.3	Loading the tooth for the largest principal stress	76
A.4	Stress at the Lewis point	78
A.5	Stresses based on the AGMA standard and Jalilvand fomula	81
	Appendix B. Computer Program - TOOTH	83
	Appendix C. Computer Program - MESH	113
	VITA	129

List of Illustrations

Figure 1. Generating a spur gear with a hob [1]	2
Figure 2. Typical tooth fracture	3
Figure 3. Profile of a gear	9
Figure 4. Profile of a pinion	10
Figure 5. Geometry of a meshed gear pair	11
Figure 6. Geometry of a meshed gear pair after the pinion rotates	12
Figure 7. The tooth coming into contact	14
Figure 8. The end of contact	16
Figure 9. Beginning of one pair of teeth in contact	18
Figure 10. End of one pair of teeth in contact	19
Figure 11. The tooth coming into contact for a pinion meshing	21
Figure 12. Loads for meshed gear model	25
Figure 13. Restraints for meshed gear model	26
Figure 14. Restraints for model of pinion meshing with rack	27
Figure 15. The distorted geometry of the tooth	29
Figure 16. Mesh of the teeth in contact	30
Figure 17. Results of mesh size study	31
Figure 18. Results of rack thickness study	33
Figure 19. Load magnitude effects	34
Figure 20. Plot of tensile stress versus angle for model group L ($N_p:20/N_g:20$)	39
Figure 21. Plot of tensile stress versus angle for model group M ($N_p:20/N_g:40$)	41

Figure 22. Plot of tensile stress versus angle for model group N ($N_p:20/N_G:60$)	43
Figure 23. Plot of tensile stress versus angle for model group O ($N_p:20/N_G:100$)	45
Figure 24. Plot of tensile stress versus angle for model group O ($N_p:20/N_G:\infty$)	47
Figure 25. Meshing process of a tooth	49
Figure 26. Model for predicting the stresses	52
Figure 27. Three forces in the FEM model	65
Figure 28. Fatigue diagram	66
Figure 29. Generation of tooth profile [4]	72
Figure 30. Generation of root trochoid [10]	74
Figure 31. Load at highest point for one tooth contact [5]	77
Figure 32. Location of the Lewis point [7]	79

List of Tables

Table 1.	Model descriptions	36
Table 2.	Results for model group L ($N_p:20/N_G:20$)	38
Table 3.	Results for model group M ($N_p:20/N_G:40$)	40
Table 4.	Results for model group N ($N_p:20/N_G:60$)	42
Table 5.	Results for model group O ($N_p:20/N_G:100$)	44
Table 6.	Results for model group P ($N_p:20/N_G:\infty$)	46
Table 7.	Results for model group Q ($N_p:30/N_G:30$)	50
Table 8.	Results for model group Q ($N_p:40/N_G:40$)	51
Table 9.	Results for model group L ($N_p:20/N_G:20$)	54
Table 10.	Results for model group M ($N_p:20/N_G:40$)	55
Table 11.	Results for model group N ($N_p:20/N_G:60$)	56
Table 12.	Results for model group O ($N_p:20/N_G:100$)	57
Table 13.	Results for model group P ($N_p:20/N_G:\infty$)	58
Table 14.	Results for model group T1 ($N_p:18/N_G:100$)	60
Table 15.	Results for model group T2 ($N_p:24/N_G:42$)	61
Table 16.	Results for model group T3 ($N_p:37/N_G:59$)	62

Nomenclature

a	addendum
b	dedendum
h	height of load above Lewis point
K_D	stress concentration factor calculated from Dolan and Broghamer formula
K_J	stress concentration factor calculated from Jalilvand formula
N_G, N_2	number of teeth of the gear (driven)
N_P, N_1	number of teeth of the pinion (driver)
P	diametral pitch
R	standard pitch radius
R_b	base radius
R_c	radius from center of gear to apex of parabola
R_o	addendum radius
R_X	radius from center of gear to point on involute at end of contact
r_f	fillet radius on hob tip
S_L	tensile stress at Lewis point
S_R	normal stress at Lewis point
σ_t	maximum stress at the fillet

t	tooth thickness at Lewis point
W	tangential load
W_c	tensile force caused by coincident points
W_R	radial load
X_A, Y_A	coordinates of point A on the involute
X_D, Y_D	coordinates of point D on addendum circle
X_E, Y_E	coordinates of point E on the trochoid
X_G, Y_G	coordinates of point on the gear
X_L, Y_L	coordinates of point on Lewis point
X_P, Y_P	coordinates of point on the pinion
X_R, Y_R	coordinates of point on dedendum circle
α	approach angle
β	recess angle
θ_B	beginning angle for one pair of teeth in contact
θ_E	end angle for one pair of teeth in contact
φ	pressure angle
φ_L	angle between action line and horizontal line
σ	combined stress calculated at Lewis point
σ_{FEM}	maximum tensile stress calculated from finite element method
σ_{AGMA}	maximum tensile stress calculated from AGMA standard
σ_{Jal}	maximum tensile stress calculated from Jalilvand's formula

1.0 Introduction

This is a study of bending stress variation at the root fillet of the meshed gear pairs during the approach and recess action of a pinion tooth.

Modern spur gears are generated to produce an involute tooth profile. The most common method for generating modern spur gears is the hobbing method. The principle of the hobbing method is illustrated for cutting external gears in Fig. 1 [1]. In this study, all the gear teeth are generated with the hobbing method.

As power is transmitted from a pinion to a gear (or rack), the load is carried by the teeth in contact. Therefore, there exist bending stresses at the root fillets and contact, or Hertzian, stresses around the contact areas. The focus in this study is on the bending stresses.

Many investigators have noted that the stresses at the fillet of the compression side of the gear tooth are larger than those on the tension side of the tooth, however, there is no fatigue under compressive stresses. The great majority of broken gears teeth show the fracture line extending from the fillet on the compression side into the gear blank and up and out on the tension side of the tooth above the fillet as indicated in Fig. 2 [2]. Therefore, it is important to know the bending stresses

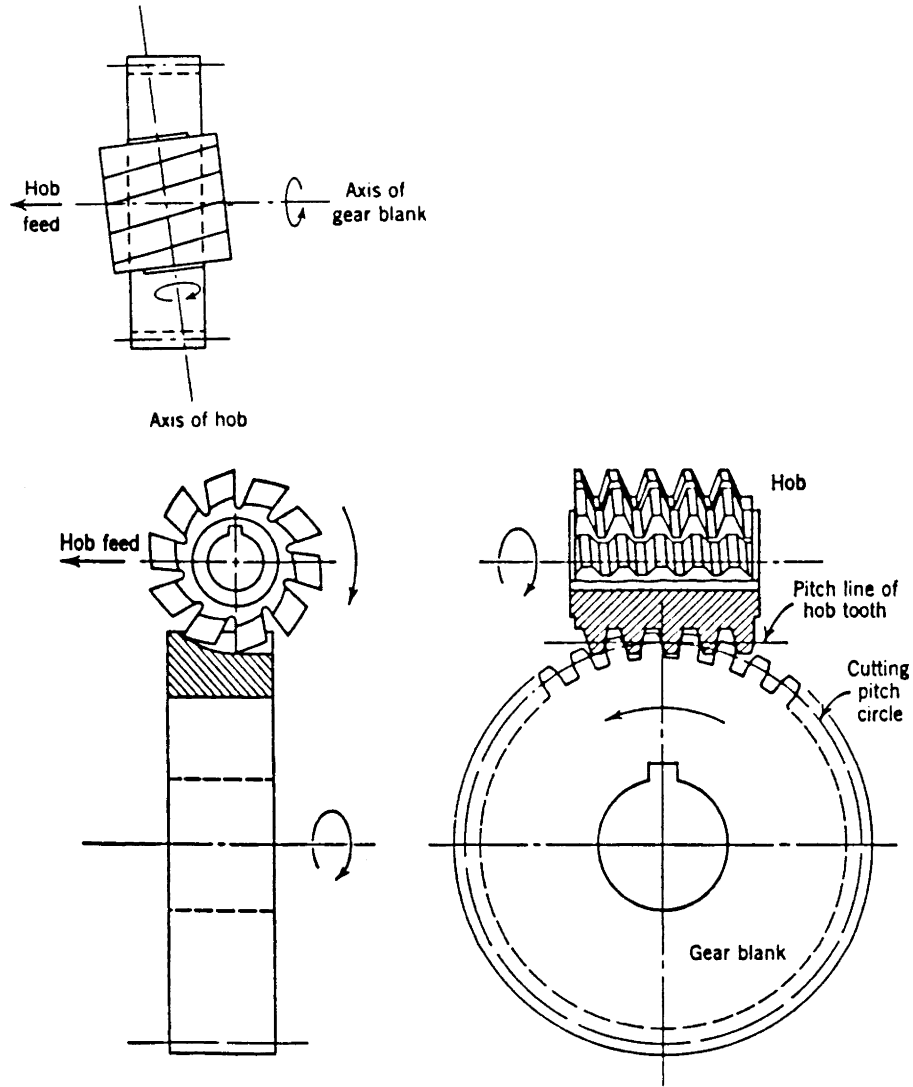


Figure 1. Generating a spur gear with a hob [1]

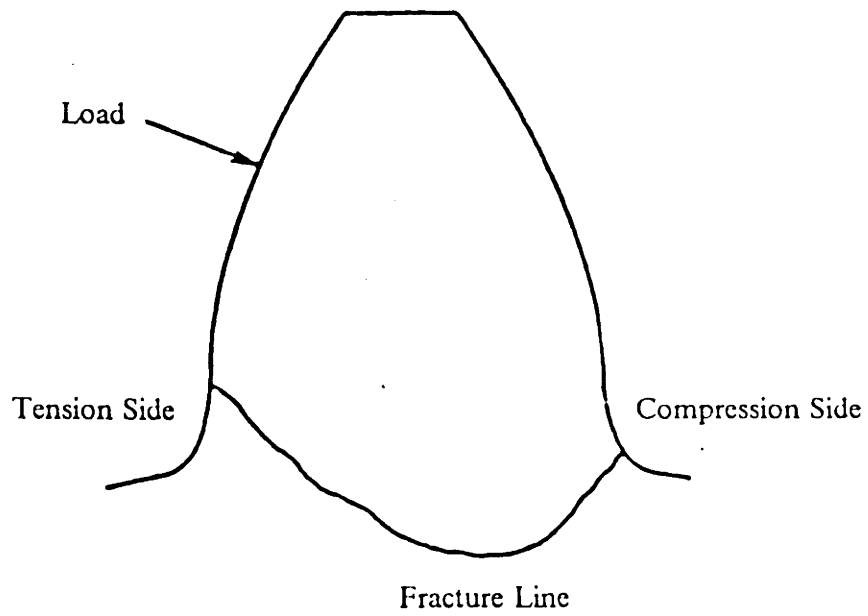


Figure 2. Typical tooth fracture

in the fillet and the variation of these bending stresses as the tooth moves through the meshing process.

A number of investigations have been made to relate stresses at the root fillet to the tooth geometry. Wilfred Lewis [3] inscribed a parabola within the tooth profile and modeled the tooth as a beam of uniform strength. The Lewis method has been incorporated into the American Gear Manufacturers Association (AGMA) design standards and is still the basis for most current designs. Jalilvand [4] used the results obtained from finite element analyses to perform a multiple linear regression analysis that predicts the stress concentration factor at the theoretical weakest point. Both AGMA and Jalilvand predicted the maximum tensile stress during mesh, however, during the duration of contact, the tensile stress on the fillet root is not steady. In order to predict the failure on the fillet root due to the tensile stress more accurately, it is necessary to describe the tensile stress change on the fillet root during the duration of contact.

Jalilvand [4] analytically described the points along the tooth profile in his study. In Chapter 3, the geometry of a meshed gear pair was defined by coordinate translation and rotation.

SUPERTAB [5] and SUPERB [6] are two computer programs which are used to generate and analyze the gear models. Chapter 4 discusses the techniques in such modeling.

2.0 Literature Review

One of the earliest investigators who attempted to relate the tensile stress to the geometry of the tooth was Wilfred Lewis [3]. In 1892, Lewis used beam theory by inscribing a parabola within the tooth profile to represent a cantilever beam of uniform strength. The point of tangency of the parabola to the tooth root was described as theoretical weakest location.

In 1942, Dolan and Broghamer [7] used photoelastic techniques to analyze the maximum tensile stress developed in the root of spur gear teeth. From their results, Dolan and Broghamer noted that the location of the maximum stress obtained was not greatly different than the theoretical weakest point determined by Lewis. In Dolan and Broghamer's model, the concentrated load was applied to the flank of the tooth. Dolan and Broghamer simplified the root form as a fillet of constant curvature. Using the Lewis theory, Dolan and Broghamer compute the tensile stress at the root and condensed their results into two equations which gave the stress concentration factor K_D as:

$$K_D = 0.22 + \left(\frac{t}{r}\right)^{0.2} \left(\frac{t}{h}\right)^{0.4}$$

for a 14.5 degree pressure angle, and

$$K_D = 0.18 + \left(\frac{t}{r}\right)^{0.15} \left(\frac{t}{h}\right)^{0.45}$$

for a 20 degree pressure angle, where

t: thickness of tooth at Lewis' theoretical weakest section

r: fillet radius

h: height of load position above the Lewis point

The work of Lewis, Dolan and Broghamer has become the standard for design in the American Gear Manufactures Association (AGMA) [8].

With the help of a modern digital computer, it is possible to analyze gear tooth models via the finite element method. In 1973, Wilcox and Coleman [9] used finite element analysis to compute the gear tooth stresses. Their results compared favorably with those obtained from Dolan and Broghamer formula.

Mitchiner and Mabie [10] presented a method for the numerical computation of the Lewis form factor and stress for hobbled spur gear teeth. With this analytical determination of the Lewis form factor, the difficulties of the graphical method and the limitations of the chart method were eliminated.

Jalilvand [4] used the finite element method to investigate the effects of undercutting in spur gear teeth. Jalilvand validated his work by analyzing the Dolan and Broghamer's photoelastic model. His results compared well with those of Dolan and Broghamer.

All of the earlier investigations focused on the maximum tensile stress at the fillet root. As the result of the literature review, it was noted that no treatment is made for the tensile stress variation at the root fillet of the tooth during the duration of contact.

3.0 Geometry Modeling of Meshed Spur Gear Pairs

3.1 Introduction

In order to use SUPERTAB [5], a finite element modeling and analysis program, to create finite element models, it is necessary to define the geometry of a meshed gear pair. In this study, the geometric description of a meshed gear pair was written as a universal file. In order to describe the duration of contact, the approach angle and recess angle are defined and the contact ratio is also discussed in this chapter.

3.2 Using TOOTH [Appendix B] to generate meshed spur gear models

TOOTH [Appendix B] is a computer program which generates a data file, a geometric description of the profile of a gear tooth. This study used coordinate translation and rotation to define the geometry of a meshed gear pair and combined the data files of a pinion and a gear into the data file of a meshed gear pair.

Fig. 3 and 4 show the profiles of a gear and a pinion with the center at $C_1, (0, 0)$. Now, the center of the gear is transferred to C_2 , where

$$X_{C_2} = 0 \quad [3.1]$$

$$Y_{C_2} = \frac{N_1 + N_2}{P} \quad [3.2]$$

Then, the gear is rotated $(\pi + \frac{\pi}{N_2})$ with center at C_2 . After that, the data files of the gear and the pinion are combined into a data file of the meshed gear pair. Fig. 5 shows a meshed gear pair.

Now, consider the rotation of the pinion through an angle θ . Using coordinate rotation, the new coordinates of the points on the gear and the pinion can be calculated. Fig. 6 shows a meshed gear pair that the pinion was rotated an angle θ from the neutral position, or the position where the centerline of a pinion tooth coincided with the line of centers.

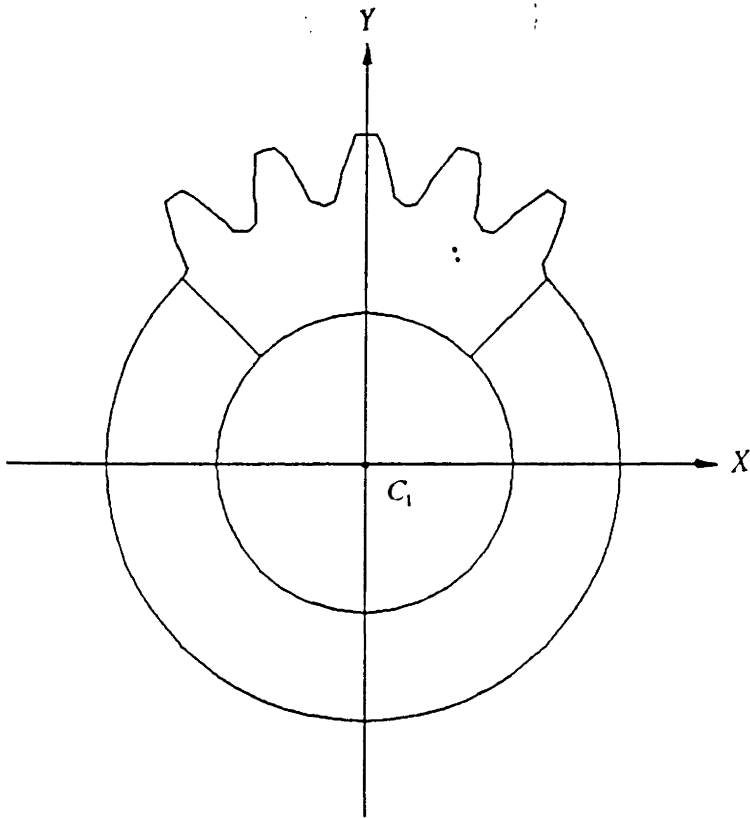


Figure 3. Profile of a gear

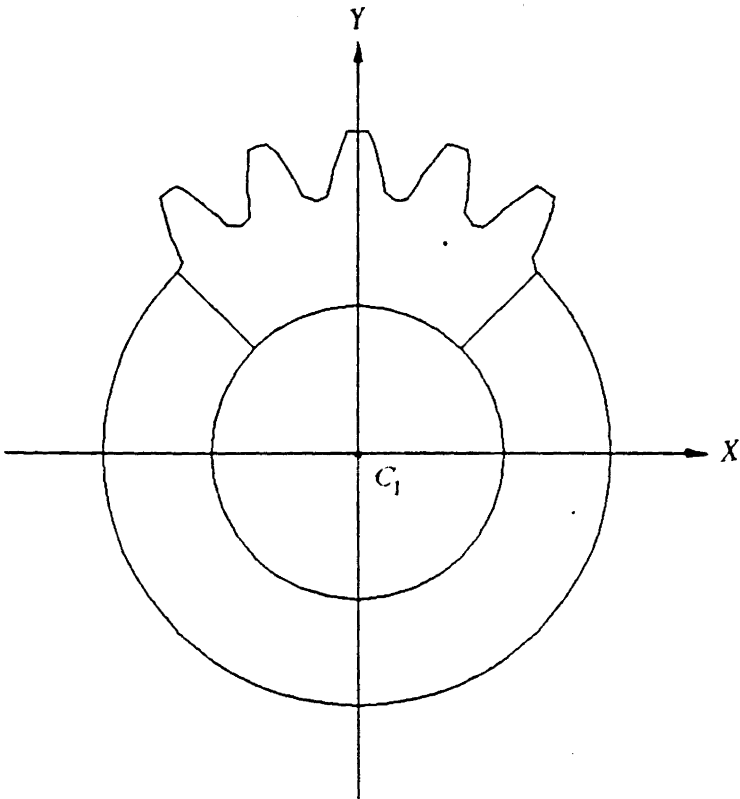


Figure 4. Profile of a pinion

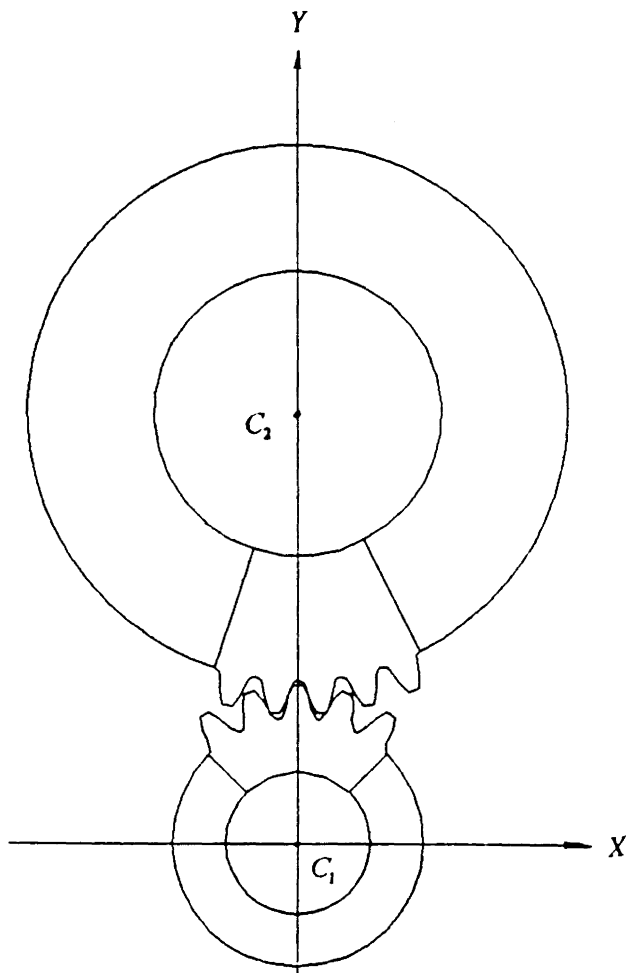


Figure 5. Geometry of a meshed gear pair

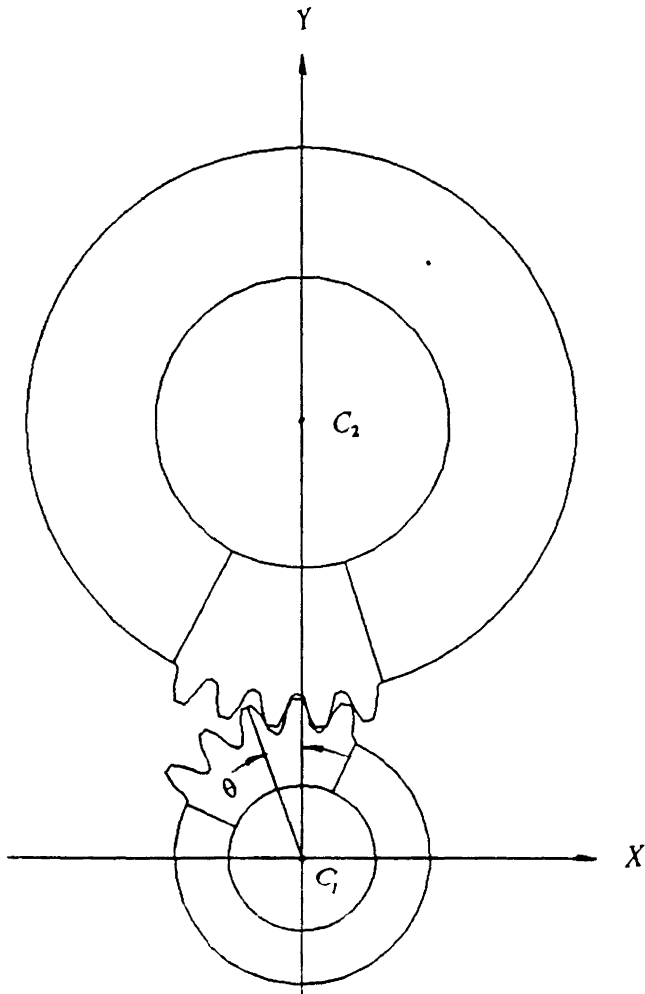


Figure 6. Geometry of a meshed gear pair after the pinion rotate

3.3 Duration of contact

In order to discuss the variation in bending stresses at the tooth root from beginning to end of contact, it is necessary to calculate angles of approach and recess. In this study, the angle of approach (recess) is defined as the angle between the line of centers and the centerline of the tooth that is coming to contact (that is leaving from contact) according to the pinion with the center at origin (0, 0). Fig. 7 shows the condition of a pinion tooth coming to contact.

$$BP = \sqrt{R_{O2}^2 - R_{b2}^2} - R_2 \sin \varphi \quad [3.3]$$

$$BC_2P = \cos^{-1} \left(\frac{R_2^2 + R_{O2}^2 - BP^2}{2R_2R_{O2}} \right) \quad [3.4]$$

In the involute tooth

$$t_B = 2R_B \left(\frac{t_A}{2R_A} + \text{inv}\varphi_A - \text{inv}\varphi_B \right) \quad [3.5]$$

Where

t_A and t_B : tooth thicknesses at R_A and R_B

So, for the gear,

$$\frac{t_{O2}}{2R_{O2}} = \frac{t_2}{2R_2} + \text{inv}\varphi - \text{inv}\varphi_{O2} \quad [3.6]$$

where

t_{O2} : tooth thickness of the gear on addendum circle

$$\varphi_{O2} = \cos^{-1} \left(\frac{R_{b2}}{R_{O2}} \right) \quad [3.7]$$

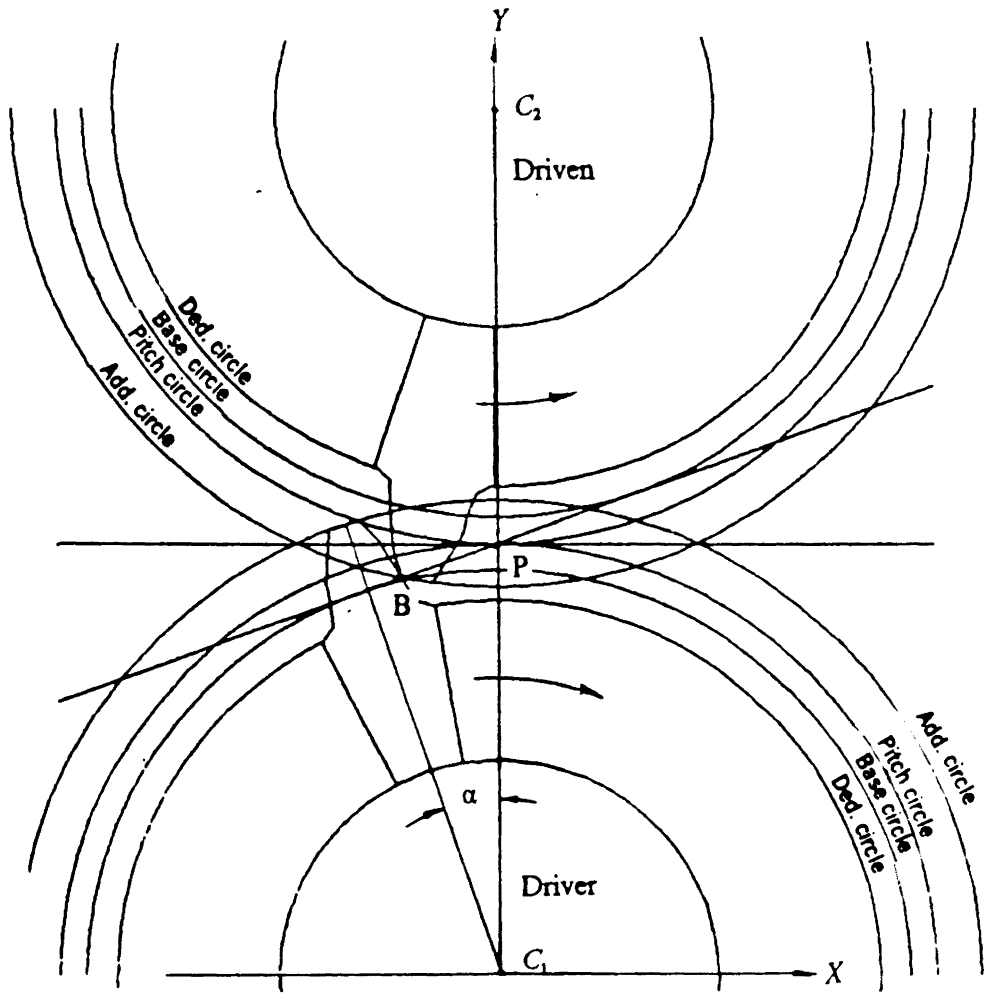


Figure 7. The tooth coming into contact

$$t_2 = \frac{\pi R_2}{N_2} \quad [3.8]$$

In this condition, the gear rotates an angle λ from the neutral position with center at C_2 , where

$$\lambda = - (BC_2P - \frac{t_{O2}}{2R_{O2}} + \frac{\pi}{N_2}) \quad [3.9]$$

This means that the pinion rotates an angle α from the line of centers with center at C_1 , where

$$\alpha = - \lambda \frac{N_2}{N_1} \quad [3.10]$$

Fig. 8 shows the condition of the end of contact.

$$AP = \sqrt{R_{O1}^2 - R_{b1}^2} - R_1 \sin \varphi \quad [3.11]$$

$$PC_1A = \cos^{-1} \left(\frac{R_1^2 + R_{O1}^2 - AP^2}{2R_1R_{O1}} \right) \quad [3.12]$$

$$\frac{t_{O1}}{2R_{O1}} = \frac{t_1}{2R_1} + inv\varphi - inv\varphi_{O1} \quad [3.13]$$

where

t_{O1} : tooth thickness of the pinion on addendum circle

$$\varphi_{O1} = \cos^{-1} \left(\frac{R_{b1}}{R_{O1}} \right) \quad [3.14]$$

$$t_1 = \frac{\pi R_1}{N_1} \quad [3.15]$$

This means that the pinion rotates an angle β from the line of centers with center at C_1 , where

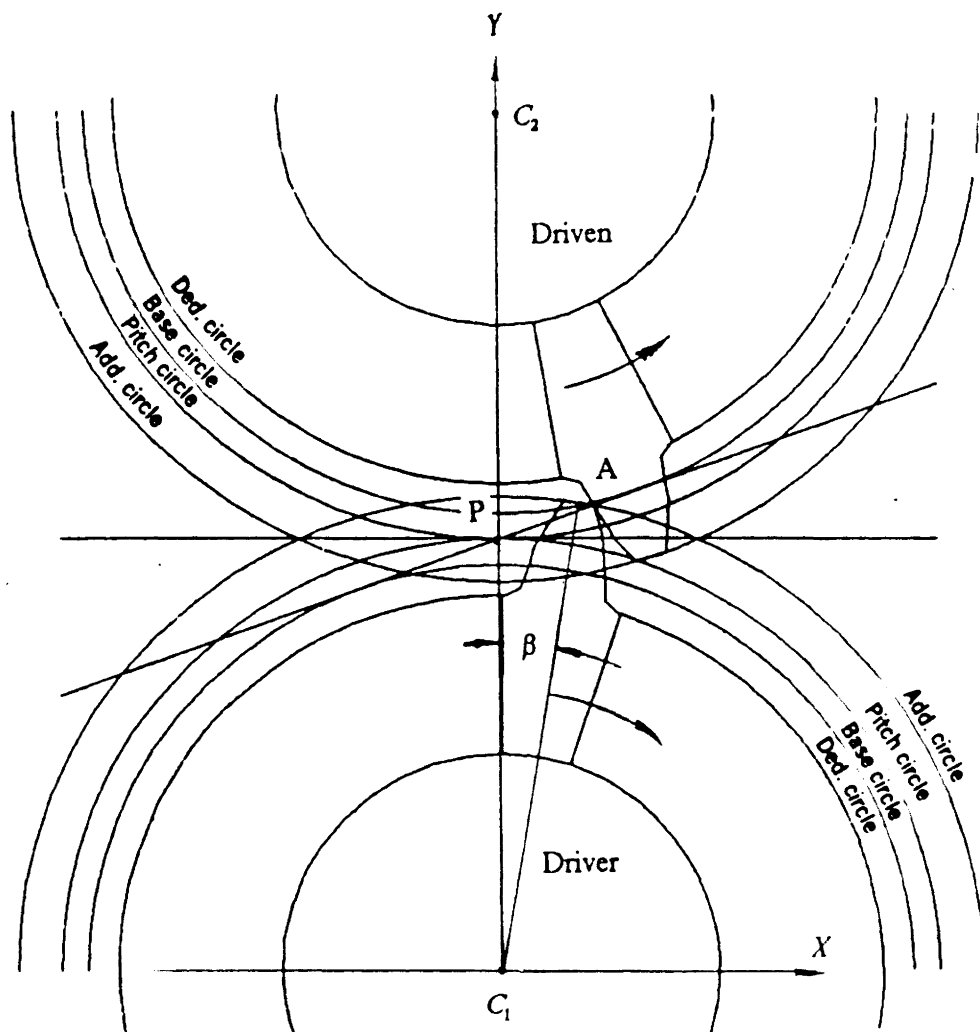


Figure 8. The end of contact

$$\beta = PC_1A - \frac{t_{O1}}{2R_{O1}} \quad [3.16]$$

3.4 Contact ratio

An equation for the length of action, Z , can be defined from Fig. 7 and 8 [1].

$$\begin{aligned} Z &= AP + BP \\ &= \sqrt{R_{O1}^2 - R_{b1}^2} + \sqrt{R_{O2}^2 - R_{b2}^2} - \frac{N_1 + N_2}{P} \sin \varphi \end{aligned} \quad [3.17]$$

The contact ratio is defined as:

$$m_p = \frac{Z}{P_b} \quad [3.18]$$

where

$$P_b = \frac{2\pi R_b}{N} \quad [3.19]$$

Considered physically, the contact ratio is the average number of teeth in contact. If the ratio is between 1.0 and 2.0, that means that there are alternatively one pair and two pairs of teeth in contact. In this case, one pair of teeth in contact occurs between angles θ_B and θ_E , where

$$\theta_B = \beta + \frac{2\pi}{N_1} \quad [3.20]$$

$$\theta_E = \alpha - \frac{2\pi}{N_1} \quad [3.21]$$

as shown in Fig. 9 and 10.

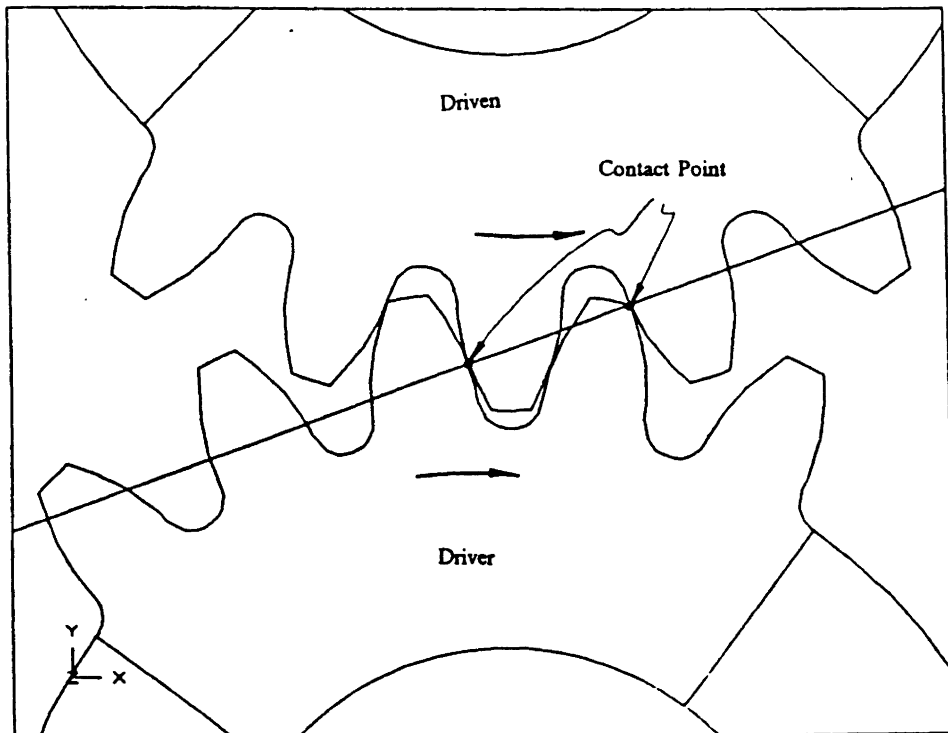


Figure 9. Beginning of one pair of teeth in contact

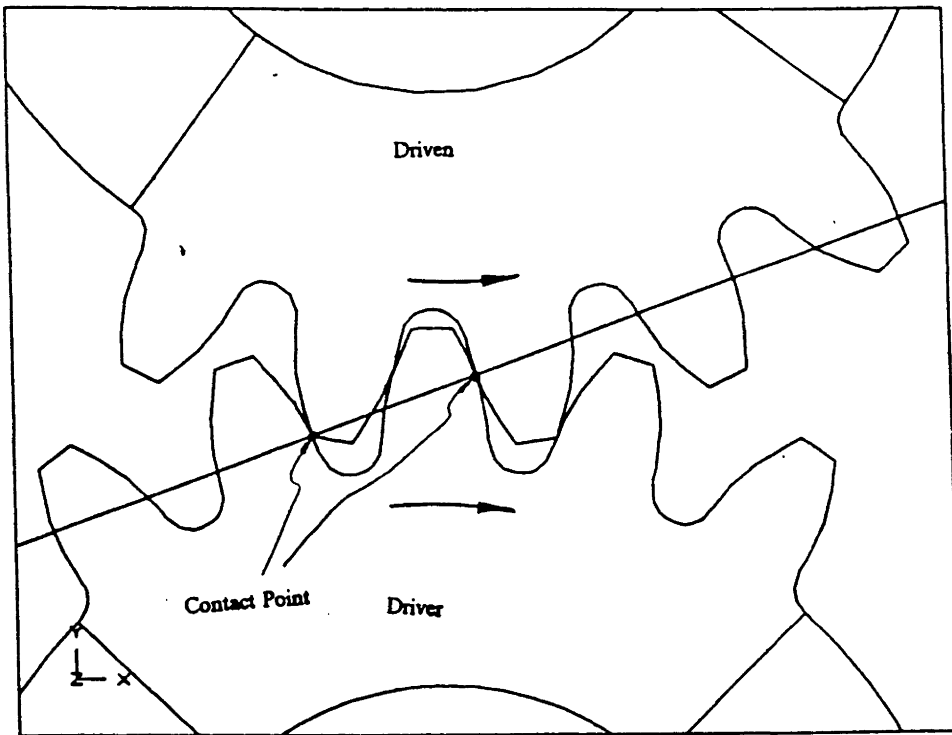


Figure 10. End of one pair of teeth in contact

3.5 Model for a pinion meshing with a rack

Now, consider the case that a pinion meshes with a rack instead of a gear. Using the same procedure as that in section 3.2, the recess angle β can be calculated. In Fig. 11, point A moved a distance AC from the neutral position to the approaching position, where

$$AC = \frac{a}{\tan \varphi} + \frac{\pi}{4P} + a \tan \varphi \quad [3.22]$$

So, the approach angle can be calculated as:

$$\alpha = \frac{2ACP}{N_1} \quad [3.23]$$

And there is just one pair of teeth in contact between θ_B and θ_E , where

$$\theta_B = \beta + \frac{2\pi}{N_1} \quad [3.24]$$

$$\theta_E = \alpha - \frac{2\pi}{N_1} \quad [3.25]$$

The equation for the length of action for a rack and pinion can be derived as

$$Z = \sqrt{R_{O1}^2 - R_{b1}^2} - R_1 \sin \varphi + \frac{a}{\sin \varphi} \quad [3.26]$$

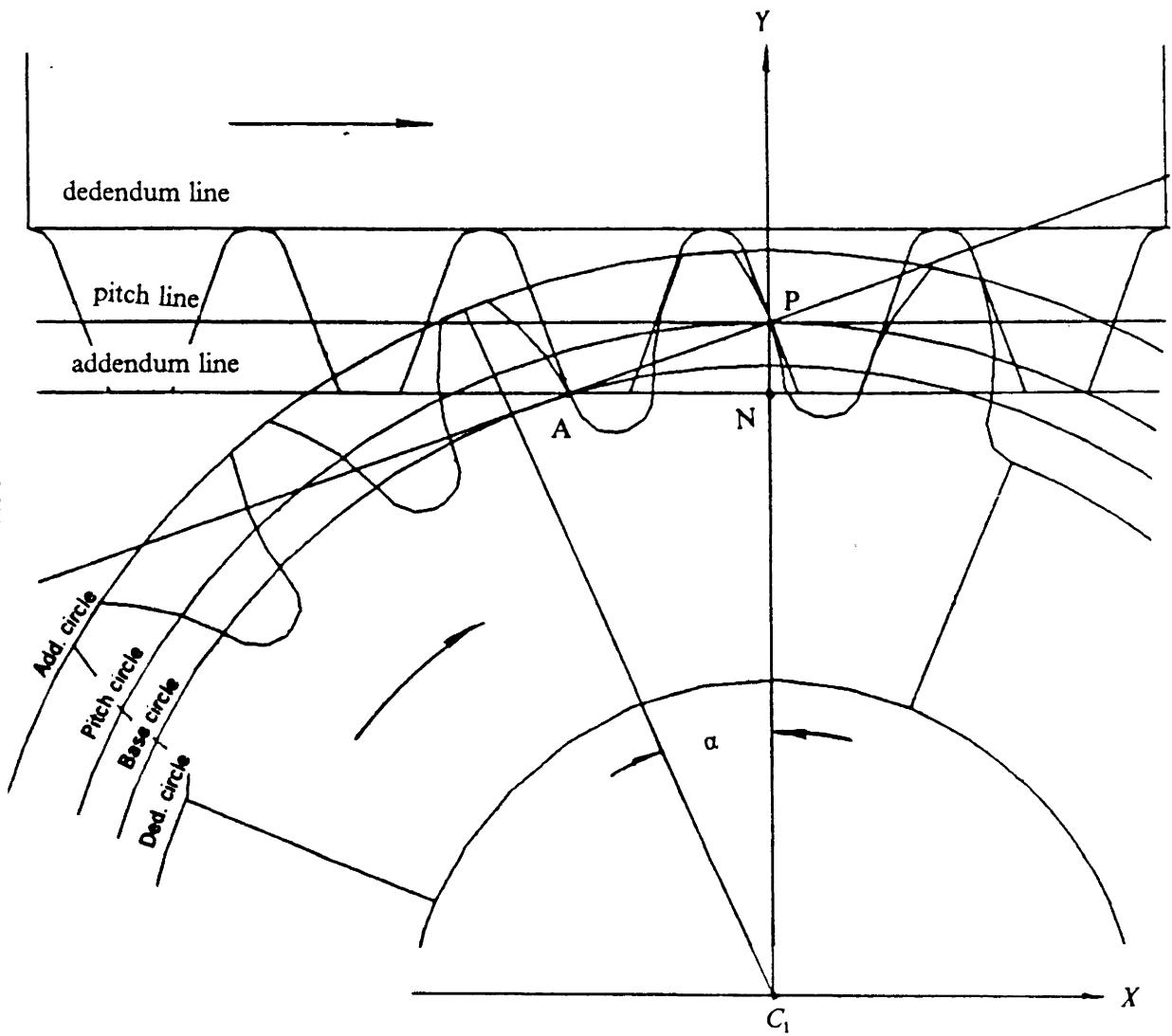


Figure 11. The tooth coming into contact for a pinion meshing with a rack

3.6 SUPERTAB

SUPERTAB is a finite element modeling and analysis program. As a pre-processor, it allows the user to create two- or three-dimensional finite element models. As an analysis program, it allows the user to perform a static or dynamic analysis and automatically stores the results in SUPERTAB database. SUPERTAB is a product of General Electric CAE International Inc. [5].

After definition of the geometry of a meshed gear pair, a model was created by joining arcs, splines, and lines created by the program in Appendices B and C.

The next step was the use of Enhanced Mesh Generation (EMG) of SUPERTAB to set the material and physical properties and generate the mesh. The user may control the mesh density. In the case of a pinion meshing with a gear or rack, it is necessary to have a finer mesh around the area of the teeth in contact and the root of the teeth in mesh. After that, Model Creation was used to apply the loads and set the restraints. The mesh size and boundary conditions will be discussed in later section.

Finally, a SUPERTAB file was written for the analysis of the finite element models.

3.7 SUPERB

SUPERB , another product of GE/CAE, is a program which performs a finite element analysis. The finite element method (FEM) embodies the concept of physical structure represented by a model composed of a finite number of assembled subcomponents or elements. Known loads are applied to the model, then a system of equations is solved and results obtained [6].

In this study, the tooth was modeled as an assembly of plane stress elements. Stresses normal to the plane of the tooth were neglected. Quadratic plane isoparametric elements were chosen to better model the curved boundaries and to more accurately approximate the displacements. It should be pointed out that the calculated nodal stress is actually an average of the stresses located at the nearest Gauss point [6].

The results of the SUPERB analysis were recorded in a listing file, listing averaged nodal stresses by descending maximum principal stresses and a plot file, containing the stress contour and distorted geometry.

4.0 Finite Element Modeling and Analysis

4.1 Modeling

Jalilvand [4] investigated several types of gear models and noted that a whole gear model, a model with a 360° ring with a few attached teeth, produced the most reliable results in comparison to Dolan and Broghamer model. The whole gear model in Jalilvand's research is a ring of unit depth that has three teeth. In this study, the pinion was rotated from the approach angle to the recess angle, so the whole gear model with five teeth was used instead of that with three teeth.

A unit torque (1 lbf-ft) was applied on the pinion in the form of nodal forces distributed on the nodes around the hole of the pinion as shown in Fig. 12.

The nodes around the hole of the gear were fixed in both x and y directions and the nodes around the hole of the pinion were fixed in radial direction as shown in Fig. 13. For the case where the driven part was a rack instead of gear, the nodes along the back of the rack were fixed in x and y direction as shown in Fig. 14.

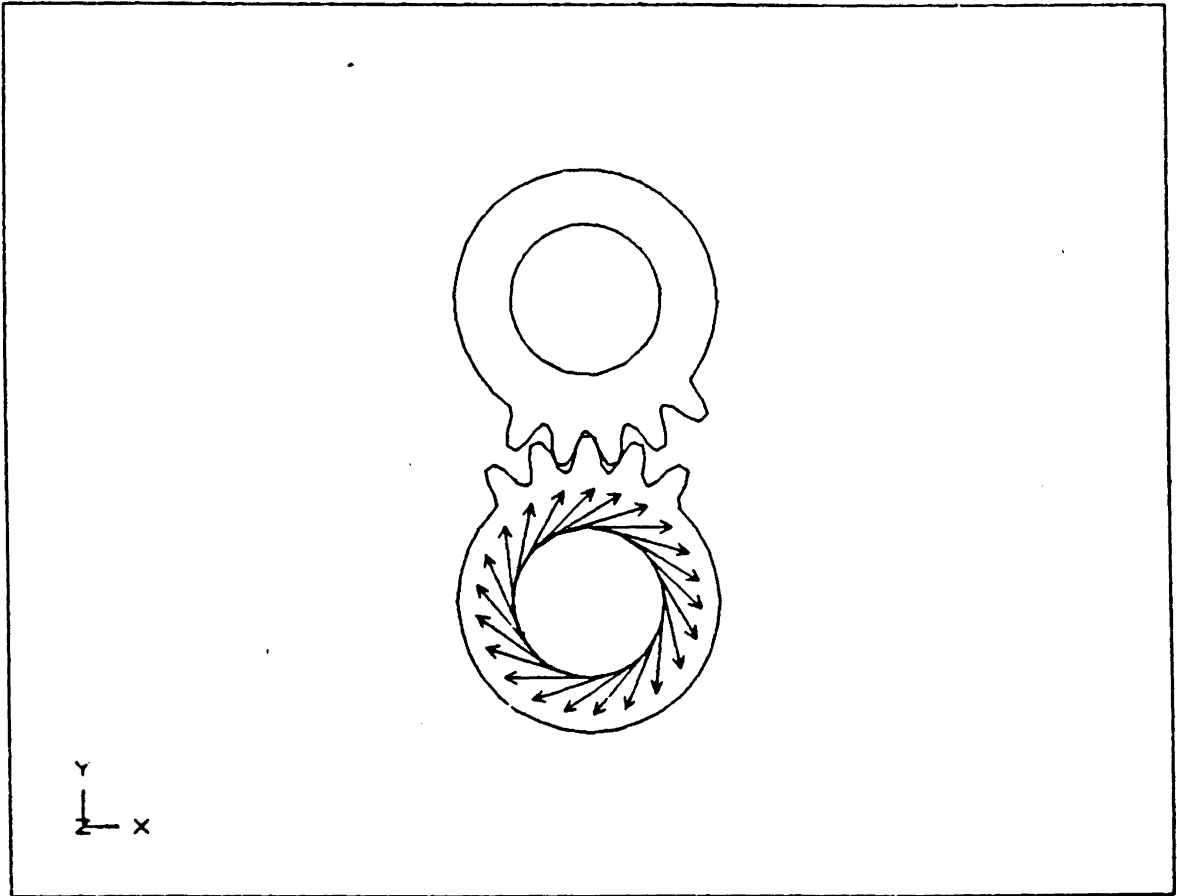


Figure 12. Loads for meshed gear model

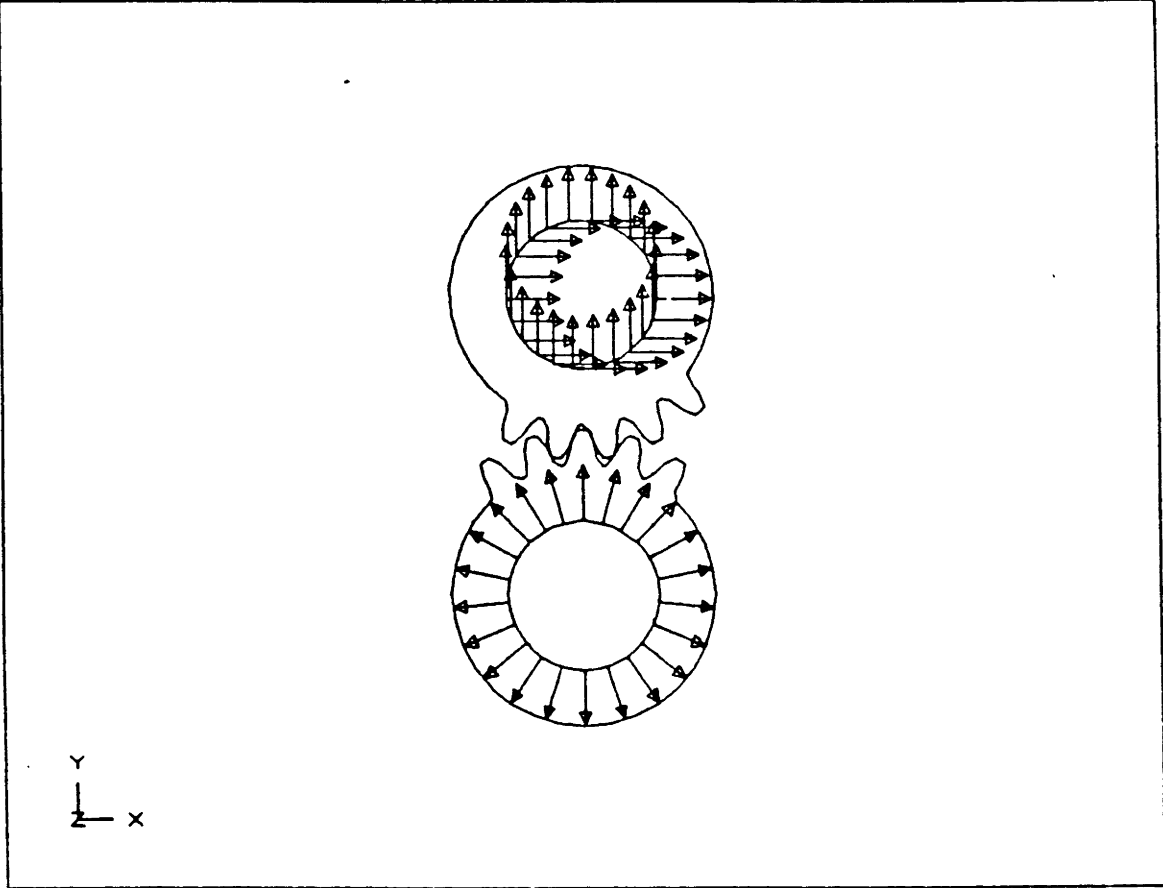


Figure 13. Restraints for meshed gear model

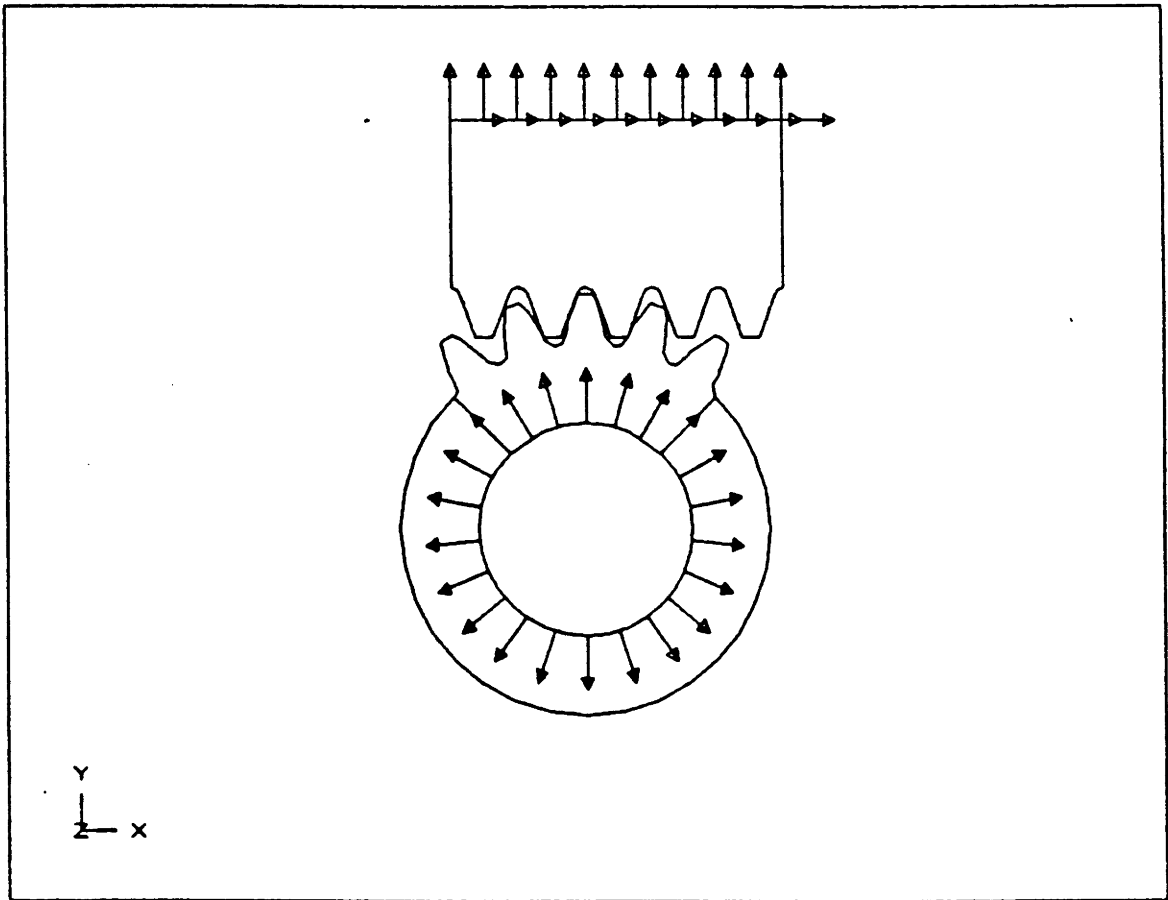


Figure 14. Restraints for model of pinion meshing with rack

In order to transmit the torque from the driver pinion to the driven gear (or rack), the points in contact between the pinion and the gear were made coincident. These points are intersections of the action line and the tooth profile. In this study, the points were located graphically instead of calculated analytically. In order to ensure that there was no interference around the contact points after distortion, it was necessary to check the distorted geometry. In this study, unit torque was applied and the strain is small. Therefore, there was no interference around the contact point. As a result, one coincident point for the contact was enough for this condition. The distorted geometry is shown in Fig. 15.

4.2 Model size study

The mesh size has very profound effect upon the accuracy of the results of a finite element analysis. For convergence of the FEM solution, it is necessary to use a finer mesh around the area of the teeth in contact and the root part of the teeth in mesh as shown in Fig. 16.

A group of meshed gear models, as described in section 4.3, with same diametral pitch (1.0), addendum (1.0 in.), dedendum (1.3 in.), pressure angle (20°) and hob tip radius (0.35 in.) but different mesh sizes around the root part of the teeth in mesh were studied. The results are shown in Fig. 17. It is indicated that as the root element length gets smaller than 0.2 in., the stresses remain relatively unchanged, that is the finite element solution has converged. Therefore, the mesh size for root part of 0.2 in. is chosen in this study.

Jalilvand [4] also considered the effect of the bore of the gear and noted that the pitch to hole diameter ratios of two or more had little effect on maximum stress on the root, so this study used a pitch to hole diameter ratio of two in all models.

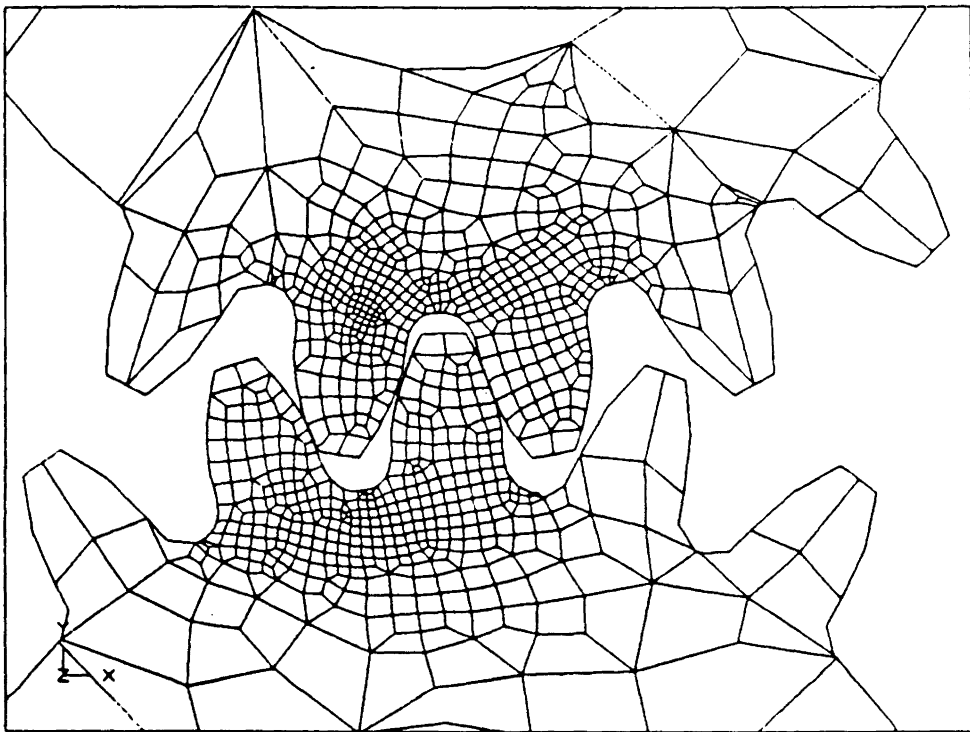


Figure 15. The distorted geometry of the tooth

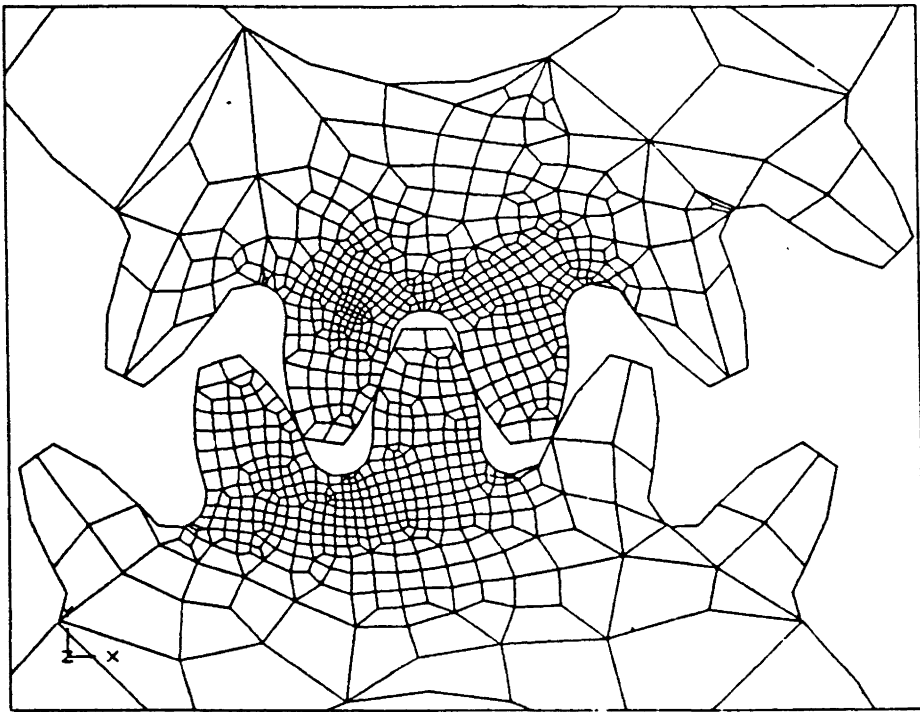


Figure 16. Mesh of the teeth in contact

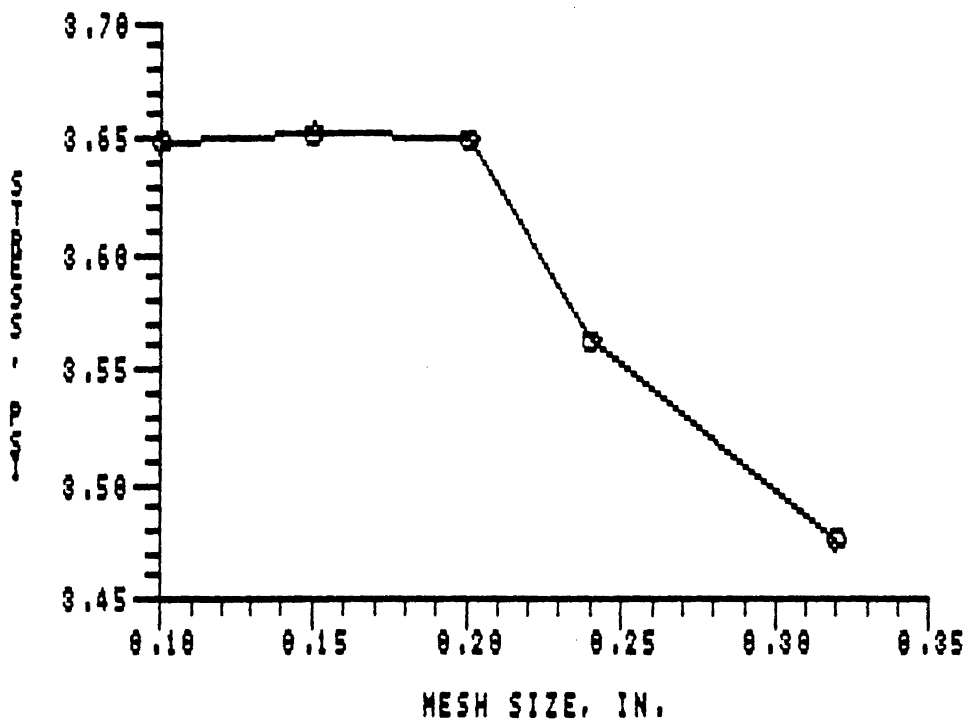


Figure 17. Results of mesh size study

In the case where the rack was used as the gear, the thickness of the rack would affect the results. Fig. 18 (same tooth size as Fig. 17) shows the results for different thicknesses of the rack. Fig. 18 indicates the stresses kept steady when the rack thickness is more than four times the tooth height. Therefore, the rack thickness was chosen as four times the tooth height.

4.3 Load magnitude effects

To determine the effect of an increasing load torque upon the pinion bending stress, the equivalent pinion bore torque was gradually increased to a level where a unit thickness steel pinion would be at the yield point in the root.

Fig. 19 shows a plot of the root bending stress as the pinion load torque is increased. The tooth size is the same as that in the previous section ($P = 1.0$, $a = 1.0$ in., $b = 1.3$ in., $r_f = 0.35$ in., $N_p = 20$, $N_g = 40$) and the mesh position is at the end of one pair of teeth in contact (for the maximum tensile stress at the root fillet). When the load is increased to 42,500 lbf-ft, the bending stress is increased to 150,000 psi (yield strength steel) linearly. In this condition, no interference around the contact point occurs. Therefore, the model of one coincident node for the contact can be used to calculate the tensile bending stress at the tooth root in the whole design range (up to the yield strength of steel, 150,000 psi).

4.4 Description of models

In this study, 10 model groups were analyzed. All the model groups, diametral pitch (1.0), addendum (1.0 in.), dedendum (1.3 in.), pressure angle (20°) and hob tip radius (0.35 in.) were fixed.

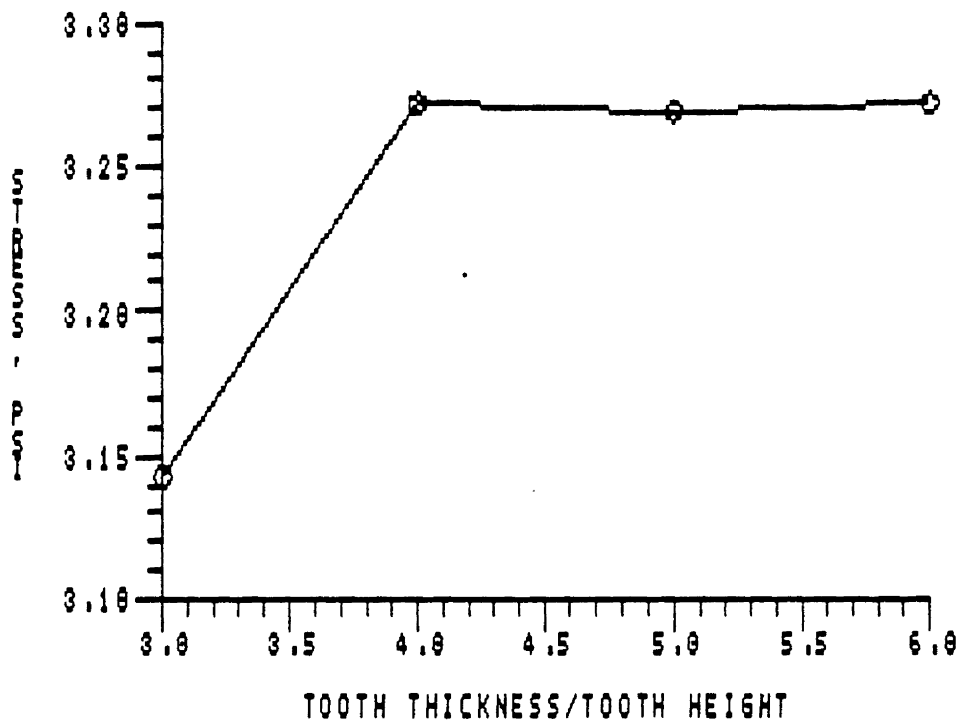


Figure 18. Results of rack thickness study

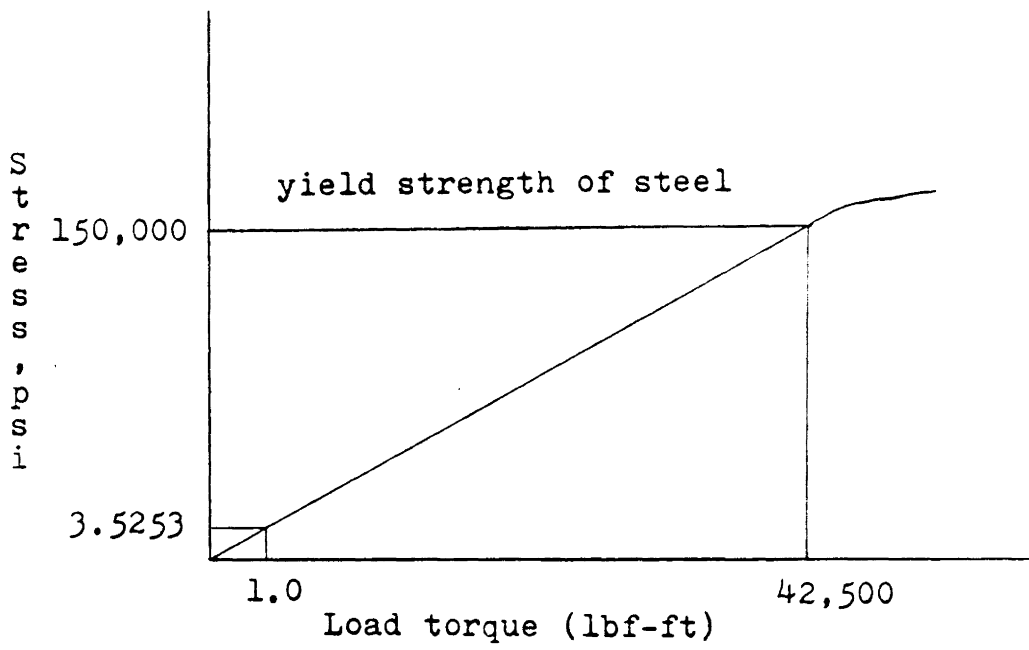


Figure 19. Load magnitude effects

Table 1 shows the model descriptions of the models. α (approach angle), β (recess angle), θ_b (beginning angle of one pair of teeth in contact), θ_E (end angle of one pair of teeth in contact) and m_p (contact ratio) can be calculated according to the equations in Chapter 3 since diametral pitch, addendum, dedendum, pressure angle, hob tip radius and numbers of teeth of the pinion and the gear (N_p and N_G) are known.

Table 1. Model descriptions

Model-group	N_P	N_G	α	β	θ_B	θ_E	m_p
L	20	20	18.5116	-9.5116	8.4884	0.5116	1.5568
M	20	40	19.9218	-9.5116	8.4884	1.9218	1.6353
N	20	60	20.5624	-9.5116	8.4884	2.5624	1.6708
O	20	100	21.1725	-9.5116	8.4884	3.1725	1.7047
P	20	$\infty(*)$	22.3273	-9.5116	8.4884	4.3273	1.7688
Q	30	30	12.9211	-6.9211	5.0789	0.9211	1.6535
R	40	40	9.9609	-5.4609	5.5391	0.9609	1.7135
T1	18	100	23.5252	-10.2977	9.7023	3.525	1.6911
T2	24	42	16.672	-8.2743	6.7357	1.672	1.6624
T3	37	59	11.102	-5.8283	3.9015	1.3722	1.7401

(*): Rack

5.0 Results

Five groups of model, L, M, N, O and P, were used to calculate σ_r (tensile stress at root fillet) and determine the relation between θ (angle of the pinion from the neutral position) and σ_r when the number of teeth of the pinion, diametral pitch, addendum, dedendum, pressure angle and hob tip radius were fixed. The results, σ_r , were listed in Table 2, 3, 4, 5 and 6. The maximum tensile stresses calculated from the finite element method, σ_{FEM} , were also listed to compare with those calculated from AGMA standards and Jalilvand's formula, σ_{AGMA} and σ_{Jal} . Fig. 20, 21, 22, 23 and 24. shows the plots of σ_r versus θ .

It should be pointed out that in this study, the pinion was rotated clockwise. When the pinion was at the position of approach angle, the tooth was coming into contact and in this condition, the load was shared by the tooth under consideration and the previous tooth. Then, the pinion was rotated to the position of beginning of one pair of teeth in contact. The previous tooth was leaving and there was only one pair of teeth in contact, so σ_r increased suddenly. As the pinion was rotated to the position of the end of one pair of teeth in contact, σ_r was maximum. AGMA and Jalilvand only predicted tension stress for this point of maximum tensile bending stress. Then, since the next tooth pair was coming to contact, the load was shared by the tooth and the later tooth and σ_r decreased suddenly. The tooth left from contact when the pinion was rotated to the position of recess angle

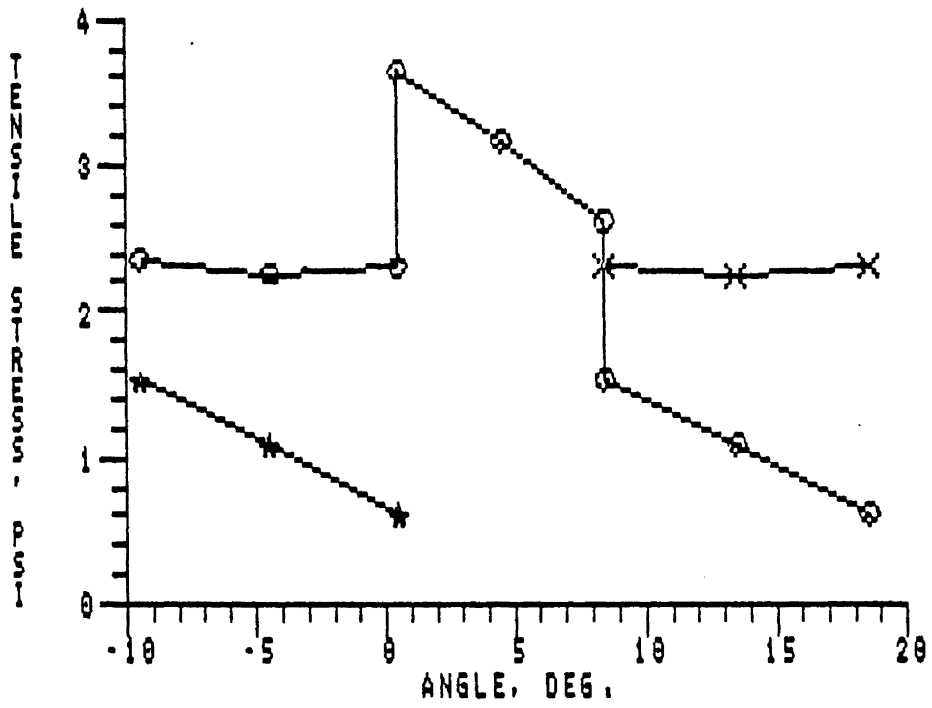
Table 2. Results for model group L ($N_p:20/N_G:20$)

Angle, degree	Tensile bending stress, σ , psi		
	Previous tooth	Driver tooth	Later tooth
18.5116	0.61789	2.3012	
13.5	1.0983	2.2435	
8.4884	1.5372	2.3134	
8.4884		2.6263	
4.5		3.1722	
0.5116		3.6497	
0.5116		2.3125	0.61223
-4.5		2.2623	1.0912
-9.5116		2.3557	1.5224

$$\sigma_{FEM} = 3.6497 \text{ psi}$$

$$\sigma_{AGMA} = 3.6950 \text{ psi}$$

$$\sigma_{Jal} = 3.66206 \text{ psi}$$



o: σ_t at the fillet of the tooth in consideration

x: σ_t at the fillet of the previous tooth

*: σ_t at the fillet of the later tooth

Figure 20. Plot of tensile stress versus angle for model group L ($N_p:20/N_G:20$)

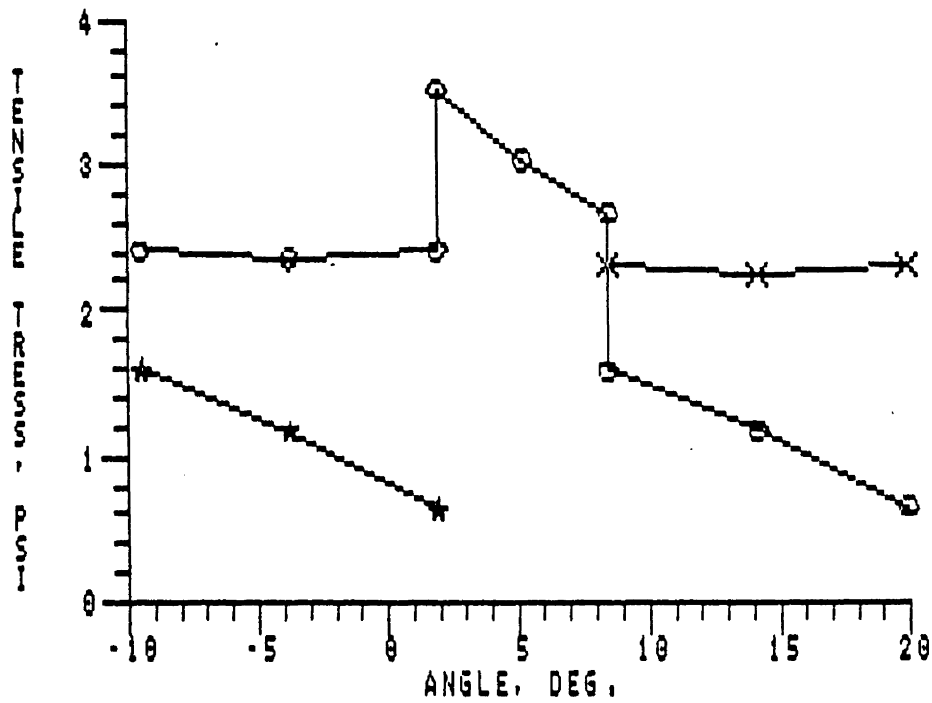
Table 3. Results for model group M ($N_p:20/N_c:40$)

Angle, degree	Tensile bending stress, σ , psi		
	Previous tooth	Driver tooth	Later tooth
19.9218	0.66024	2.3113	
14.2	1.1792	2.3058	
8.4884	1.5946	2.3264	
8.4884		2.6726	
5.2		3.0367	
1.9218		3.5253	
1.9218		2.4177	0.64212
-3.8		2.3528	1.1691
-9.5116		2.4091	1.602

$$\sigma_{FEM} = 3.5253 \text{ psi}$$

$$\sigma_{AGMA} = 3.4608 \text{ psi}$$

$$\sigma_{Jal} = 3.52326 \text{ psi}$$



- : σ_t at the fillet of the tooth in consideration
- ×: σ_t at the fillet of the previous tooth
- *: σ_t at the fillet of the later tooth

Figure 21. Plot of tensile stress versus angle for model group M ($N_p:20/N_G:40$)

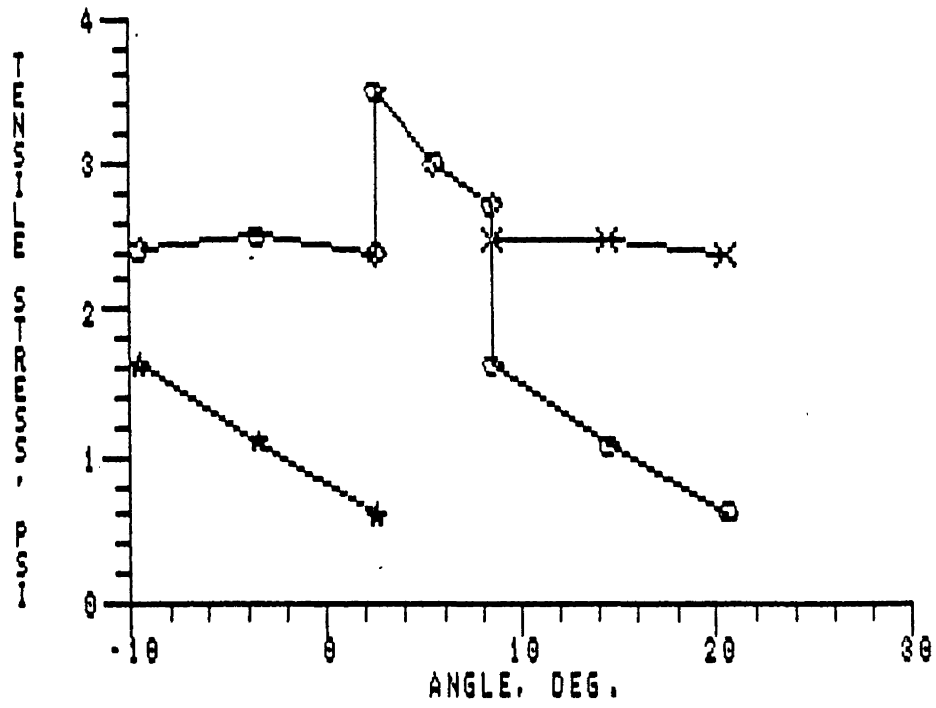
Table 4. Results for model group N ($N_p:20/N_G:60$)

Angle, degree	Tensile bending stress, σ , psi		
	Previous tooth	Driver tooth	Later tooth
20.5624	0.62326	2.3865	
14.525	1.0782	2.4915	
8.4884	1.6276	2.5032	
8.4884		2.723	
5.525		3.005	
2.5624		3.4932	
2.5624		2.3905	0.60472
-3.475		2.5138	1.1042
-9.5116		2.421	1.6335

$$\sigma_{FEM} = 3.4932 \text{ psi}$$

$$\sigma_{AGMA} = 3.4142 \text{ psi}$$

$$\sigma_{Jal} = 3.5175 \text{ psi}$$



o: σ , at the fillet of the tooth in consideration
 x: σ , at the fillet of the previous tooth
 *: σ , at the fillet of the later tooth

Figure 22. Plot of tensile stress versus angle for model group N ($N_p:20/N_c:60$)

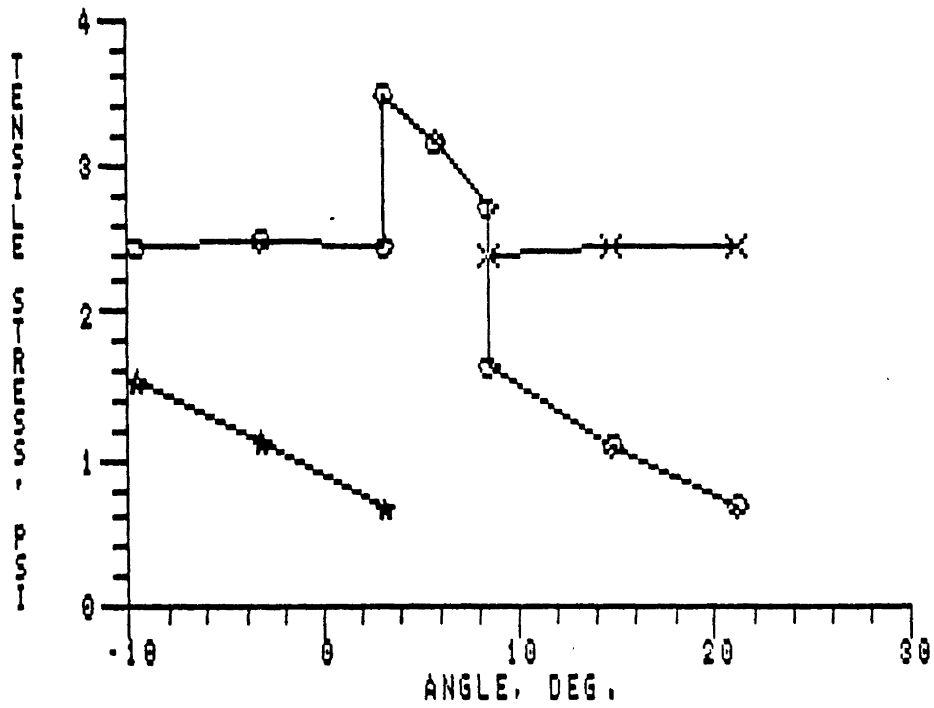
Table 5. Results for model group O ($N_p:20/N_G:100$)

Angle, degree	Tensile bending stress, σ , psi		
	Previous tooth	Driver tooth	Later tooth
21.1725	0.68921	2.4632	
14.8	1.0921	2.4513	
8.4884	1.6276	2.33891	
8.4884		2.7087	
5.8		3.1617	
3.1725		3.4833	
3.1725		2.4492	0.67325
-3.2		2.4987	1.1251
-9.5116		2.4422	1.5286

$$\sigma_{FEM} = 3.4833 \text{ psi}$$

$$\sigma_{AGMA} = 3.4015 \text{ psi}$$

$$\sigma_{Jol} = 3.4759 \text{ psi}$$



o: σ , at the fillet of the tooth in consideration

x: σ , at the fillet of the previous tooth

*: σ , at the fillet of the later tooth

Figure 23. Plot of tensile stress versus angle for model group O ($N_p:20/N_G:100$)

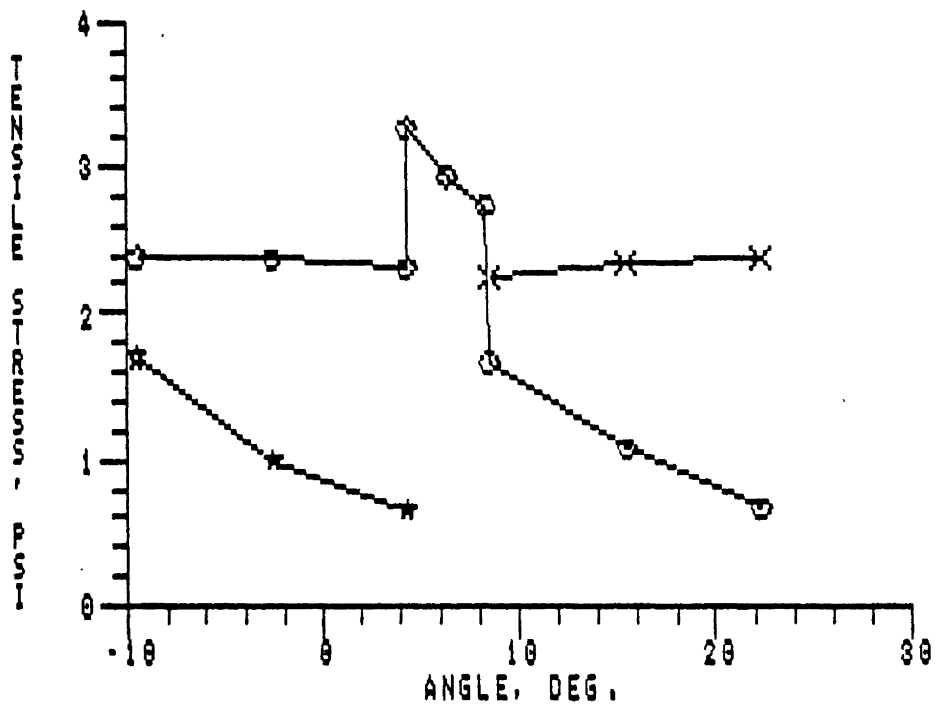
Table 6. Results for model group P ($N_p:20/N_G:\infty$)

Angle, degree	Tensile bending stress, σ_t , psi		
	Previous tooth	Driver tooth	Later tooth
22.3273	0.67318	2.3892	
15.5	1.075	2.3612	
8.4884	1.6665	2.2641	
8.4884		2.7262	
6.4		2.9358	
4.3273		3.2718	
4.3273		2.3091	0.65432
-2.6		2.3733	1.002
-9.5116		2.3852	1.7013

$$\sigma_{FEM} = 3.2718 \text{ psi}$$

$$\sigma_{AGMA} = 3.2034 \text{ psi}$$

$$\sigma_{Jal} = 3.3152 \text{ psi}$$



o: σ_f at the fillet of the tooth in consideration

x: σ_f at the fillet of the previous tooth

*: σ_f at the fillet of the later tooth

Figure 24. Plot of tensile stress versus angle for model group O ($N_p:20/N_c:$)

and at this point, the load was still shared by two teeth. Fig. 25 shows a sequence of pictures from the tooth in consideration coming to contact to the tooth leaving.

In order to determine the relation between θ and S , when N_p was not fixed, two more groups of model, Q and R, were analyzed. The results were listed in Table 7 and 8.

From the results obtained from the finite element analysis, a model for predicting the stresses during the duration of contact could be derived. Inspection of Fig. 20 to 24 reveals that the maximum bending tensile stresses are characterized by six points, σ_1 , σ_2 , σ_3 , σ_4 , σ_5 and σ_6 , and one slope, S_{34} .

Where

σ_1 : stress for the position of approach angle

σ_2 : stress for the position of beginning angle of one pair of teeth in contact when the load is shared by two teeth

σ_3 : stress for the position of beginning angle of one pair of teeth in contact when the load is carried by just one tooth

σ_4 : stress for the position of end angle of one pair of teeth in contact when the load is carried by just one tooth

σ_5 : stress for the position of end angle of one pair of teeth in contact when the load is shared by two teeth

σ_6 : stress for the position of recess angle

S_{34} : slope from σ_3 to σ_4

$$S_{34} = \frac{\sigma_4 - \sigma_3}{\theta_B - \theta_E}$$

σ_1 , σ_2 , σ_3 , σ_5 , σ_6 and S_{34} are fixed, from σ_1 to σ_2 and from σ_3 to σ_4 , the stress increases linearly and from σ_5 to σ_6 , the stress remains constant as diametral pitch, addendum, dedendum, pressure angle, hob tip radius and number of teeth of the pinion are fixed. This model is shown in Fig. 26. To ensure the reasonability of this model, the reader might compare Fig. 26 with Fig. 20, 21, 22, 23 and 24.

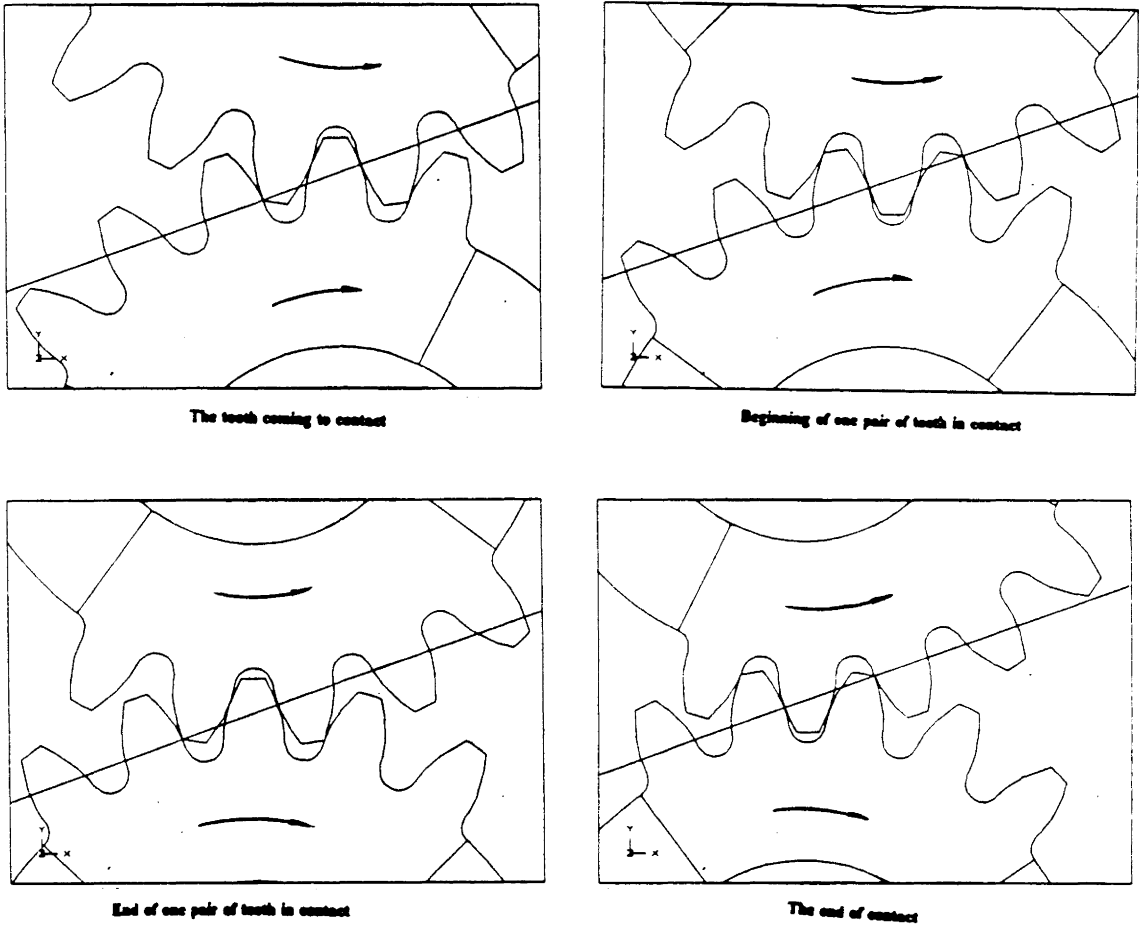


Figure 25. Meshing process of a tooth

Table 7. Results for model group Q ($N_p:30/N_g:30$)

Angle, degree	Tensile bending stress in the driver tooth, psi
12.9211	0.31539
5.0789	0.998
5.0789	1.586
0.9211	2.0637
0.9211	1.3946
-6.9211	1.4442

$$\sigma_{FEM} = 2.0638 \text{ psi}$$

$$\sigma_{AGMA} = 2.1028 \text{ psi}$$

$$\sigma_{Jol} = 2.1006 \text{ psi}$$

Table 8. Results for model group R ($N_p:40/N_c:40$)

Angle, degree	Tensile bending stress in the driver tooth, psi
9.9609	0.21735
3.5391	0.82067
3.5391	1.2639
0.9609	1.4744
0.9609	1.0398
-5.4609	1.0869

$$\sigma_{FEM} = 1.4744 \text{ psi}$$

$$\sigma_{AGMA} = 1.4494 \text{ psi}$$

$$\sigma_{Jal} = 1.4936 \text{ psi}$$

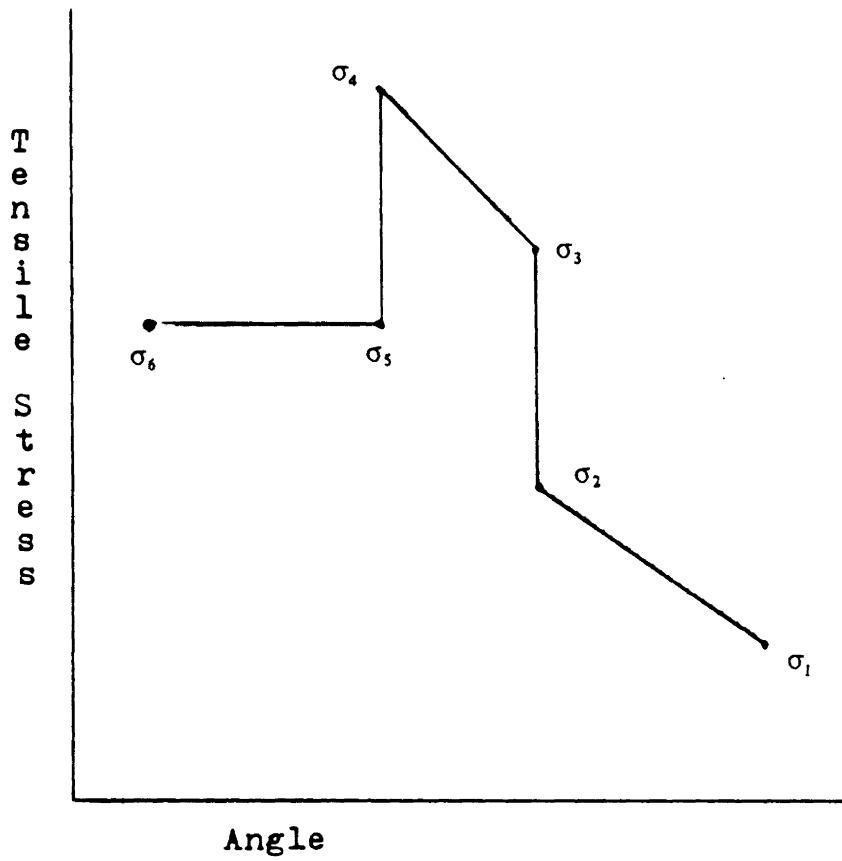


Figure 26. Model for predicting the stresses

The mean values of σ_1 , σ_2 , σ_3 , σ_5 , σ_6 and S_{34} were calculated for model L, M, N, O and P ($N_p:20$):

$$\sigma_1 = 0.65276 \text{ psi}$$

$$\sigma_2 = 1.6153 \text{ psi}$$

$$\sigma_3 = 2.6914 \text{ psi}$$

$$\sigma_5 = \sigma_6 = 2.3929 \text{ psi}$$

$$S_{34} = 0.13299$$

In order to check this prediction relationship, stresses calculated from the finite element analysis for model groups L, M, N, O and P were compared to stresses predicted by the model. The results were listed in Table 9, 10, 11, 12 and 13. The percentage differences between σ_{FEM} and σ_{pre} always keep under 6% and in most cases are less than 4%.

For model group Q ($N_p:30/N_G:30$):

$$\sigma_1 = 0.31539 \text{ psi}$$

$$\sigma_2 = 0.998 \text{ psi}$$

$$\sigma_3 = 1.586 \text{ psi}$$

$$\sigma_5 = \sigma_6 = 1.4194 \text{ psi}$$

$$S_{34} = 0.11489$$

And for model group R ($N_p:40/N_G:40$):

$$\sigma_1 = 0.21735 \text{ psi}$$

$$\sigma_2 = 0.82067 \text{ psi}$$

$$S_3 = 1.2639 \text{ psi}$$

$$\sigma_5 = \sigma_6 = 1.0664 \text{ psi}$$

$$S_{34} = 0.08165$$

So, for: $\phi = 20^\circ$, $P = 1.0$, $a = 1.0 \text{ in.}$, $b = 1.3 \text{ in.}$, $r_f = 0.35 \text{ in.}$ and the number of teeth of the pinion ranging from 18 (minimum number of teeth to avoid undercutting) to 40, σ_1 , σ_2 , σ_3 , σ_5 , σ_6 and S_{34} can be calculated by linearly interpolating. the approach angle, recess angle, beginning angle of one pair of teeth in contact and end angle of one pair of teeth in contact can be calculated from the equations in Chapter 3. Therefore, σ_4 can be calculated.

Table 9. Results for model group L ($N_p:20/N_G:20$)

Angle, degree	σ_{xx} , FEM, psi	σ_{xx} , prediction, psi	Error, percent
18.5116	0.61789	0.65276	5.64
13.5	1.0983	1.134	3.25
8.4884	1.5372	1.6153	5.08
8.4884	2.6263	2.6914	2.48
4.5	3.1722	3.2218	1.56
0.5116	3.6497	3.7522	2.81
0.5116	2.3125	2.3929	3.48
-4.5	2.2623	2.3929	5.77
-9.5116	2.3557	2.3929	2.45

Table 10. Results for model group M ($N_p:20/N_c:40$)

Angle, degree	σ_{xx} , FEM, psi	σ_{xx} , prediction, psi	Error, percent
19.9218	0.66024	0.65276	1.13
14.2	1.1792	1.1345	3.79
8.4884	1.5946	1.6153	1.3
8.4884	2.6726	2.6914	0.7
5.2	3.0367	3.1287	3.03
1.9218	3.5253	3.5647	1.12
1.9218	2.4177	2.3929	1.03
-3.8	2.3528	2.3929	1.7
-9.5116	2.4091	2.3929	0.67

Table 11. Results for model group N ($N_p:20/N_G:60$)

Angle, degree	σ_{xx} , FEM, psi	σ_{xx} , prediction, psi	Error, percent
20.5624	0.62326	0.65276	4.73
14.525	1.0782	1.1341	5.18
8.4884	1.6276	1.6153	0.76
8.4884	2.723	2.6914	1.16
5.525	3.005	3.0855	2.68
2.5624	3.4932	3.4795	0.39
2.5624	2.3905	2.3929	0.1
-3.475	2.5138	2.3929	4.81
-9.5116	2.421	2.3929	1.16

Table 12. Results for model group O ($N_p:20/N_G:100$)

Angle, degree	σ_r , FEM, psi	σ_r , prediction, psi	Error, percent
21.1725	0.68921	0.65276	5.29
14.8	1.0921	1.1363	4.05
8.4884	1.6505	1.6153	2.13
8.4884	2.7087	2.6914	0.64
5.8	3.1617	3.0489	3.57
3.1725	3.4833	3.3984	2.44
3.1725	2.4492	2.3929	2.3
-3.2	2.4987	2.3929	4.23
-9.5116	2.4422	2.3929	2.02

Table 13. Results for model group P ($N_p:20/N_c:\infty$)

Angle, degree	σ_{xx} , FEM, psi	σ_{xx} , prediction, psi	Error, percent
22.3273	0.67318	0.65276	3.03
15.5	1.075	1.1276	4.89
8.4884	1.6665	1.6153	3.07
8.4884	2.7276	2.6914	1.28
6.4	2.9358	2.9691	1.13
4.3273	3.2718	3.2448	0.83
4.3273	2.3091	2.3929	3.63
-2.6	2.3733	2.3929	0.83
-9.5116	2.3852	2.3929	2.36

As an example for the determination of the variation in pinion tooth tensile bending stresses for a pinion and gear combination not explicitly covered in the analyzed models. Suppose:

$\varphi = 20^\circ$, $P = 1.0$, $a = 1.0$ in., $b = 1.3$ in., $r_f = 0.35$ in., $N_p = 24$ and $N_G = 42$. According to the equations in Chapter 3: $\alpha = 16.672^\circ$, $\beta = -8.2743^\circ$, $\theta_B = 6.7357^\circ$ and $\theta_E = 1.6720^\circ$. σ_1 , σ_2 , σ_3 , σ_5 , σ_6 and S_{34} can be calculated by linearly interpolating:

$$\begin{aligned}\sigma_1 &= .65276 + \frac{(24 - 20)}{(30 - 20)}(.31539 - .65276) \\ &= .51781 \text{ psi}\end{aligned}$$

$$\begin{aligned}\sigma_2 &= 1.6153 + \frac{(24 - 20)}{(30 - 20)}(.998 - 1.6153) \\ &= 1.3684 \text{ psi}\end{aligned}$$

$$\begin{aligned}\sigma_3 &= 2.6914 + \frac{(24 - 20)}{(30 - 20)}(1.586 - 2.6914) \\ &= 2.2492 \text{ psi}\end{aligned}$$

$$\begin{aligned}\sigma_5 &= \sigma_6 \\ &= 2.3929 + \frac{(24 - 20)}{(30 - 20)}(1.4194 - 2.3929) \\ &= 2.0035 \text{ psi}\end{aligned}$$

$$\begin{aligned}S_{34} &= .13299 + \frac{(24 - 20)}{(30 - 20)}(.11489 - .13299) \\ &= .12575\end{aligned}$$

$$\begin{aligned}\sigma_4 &= \sigma_3 + S_{34}(\theta_B - \theta_E) \\ &= 2.886 \text{ psi}\end{aligned}$$

In order to verify the prediction model, three groups of models, T1, T2 and T3, were analyzed. The results were listed in Table 14, 15 and 16. It is indicated that the error is no more than 5%.

Table 14. Results for model group T1 ($N_p:18/N_G:100$)

Angle, degree	σ_{xx} , FEM, psi	σ_{xx} , prediction, psi	Error, percent
23.525	0.69847	0.70203	0.51
9.7023	1.6925	1.7388	2.73
9.7023	2.9048	2.8138	3.13
3.525	3.7123	3.6499	1.92
3.525	2.4894	2.5762	3.49
-10.2977	2.5988	2.5762	0.87

Table 15. Results for model group T2 ($N_p:24/N_G:42$)

Angle, degree	σ , FEM, psi	σ , prediction, psi	Error, percent
16.672	0.49342	0.51696	4.77
6.7357	1.3064	1.3684	4.74
6.7357	2.3447	2.2492	4.07
1.672	2.7943	2.8833	3.18
1.672	1.9041	1.9978	4.92
-8.2643	1.936	1.9978	3.19

Table 16. Results for model group T3 ($N_p:37/N_G:59$)

Angle, degree	σ_n , FEM, psi	σ_n , prediction, psi	Error, percent
11.102	0.24858	0.24676	0.73
3.9015	0.84967	0.87387	2.85
3.9015	1.4158	1.3589	4.02
1.3722	1.6682	1.5907	4.65
1.37222	1.16	1.1702	0.88
-5.8283	1.1285	1.1702	3.69

6.0 Conclusions and Recommendations

From the results obtained from the finite element analysis, a model for predicting the stresses during the duration of contact could be derived. The maximum bending tensile stresses are characterized by six points, σ_1 , σ_2 , σ_3 , σ_4 , σ_5 and σ_6 , and one slope, S_{34} . Where

σ_1 : stress for the position of approach angle

σ_2 : stress for the position of beginning angle of one pair of teeth in contact when the load is shared by two teeth

σ_3 : stress for the position of beginning angle of one pair of teeth in contact when the load is carried by just one tooth

σ_4 : stress for the position of end angle of one pair of teeth in contact when the load is carried by just one tooth

σ_5 : stress for the position of end angle of one pair of teeth in contact when the load is shared by two teeth

σ_6 : stress for the position of recess angle

S_{34} : slope from σ_3 to σ_4

$$S_{34} = \frac{\sigma_4 - \sigma_3}{\theta_B - \theta_E}$$

σ_1 , σ_2 , σ_3 , σ_5 , σ_6 and S_{34} are fixed, from σ_1 to σ_2 and from σ_3 to σ_4 , the stress increases linearly and from σ_5 to σ_6 , the stress remains constant as diametral pitch, addendum, dedendum, pressure angle, hob tip radius and number of teeth of the pinion are fixed. This model is shown in Fig. 26.

In the AGMA and Jalilvand models, the load is applied in the form of a concentrated force to the tooth flank along the direction of the action line. As a result, the root fillet is subjected to the tangential load, W , and the radial loads, W_R as shown in Appendix A. However, in this study, a unit torque is applied with the form of nodal forces around the bore hole of the pinion and the points in contact are made coincident. Therefore, in this study, besides W and W_R , the root fillet is subjected to the tensile stress caused by the tensile force of the coincident point, W_c , along the tangent direction of the contact point as shown in Fig. 27.

Comparing with W and W_R , W_c is very small. The nodal forces, F_x and F_y , can be calculated from the finite element method. For $a = 1.0$ in., $b = 1.3$ in., $r_f = 0.35$ in., $P = 1.0$, $N_p = 20$, $N_g = 40$ and meshing at the position for the maximum tensile stress at the root fillet (end angle for one pair of teeth in contact):

$$F_x = -1.2032 \text{ lbf}$$

$$F_y = -0.53434 \text{ lbf}$$

The forces can be decomposed to W , W_R and W_c :

$$W = 1.1932 \text{ lbf}$$

$$W_R = 0.53454 \text{ lbf}$$

$$W_c = 0.024351 \text{ lbf}$$

Therefore, the maximum tensile stresses at the root fillet calculated based on AGMA standard, Jalilvand's model and the model in this study agree with each other very well. The results based on the model in this study agree with those based on AGMA standard within 3% and 2% with those based on Jalilvand's formula.

To discuss the fatigue at the root fillet of a tooth, the modified Goodman diagram [11], as shown in Fig. 28, can be used. Where

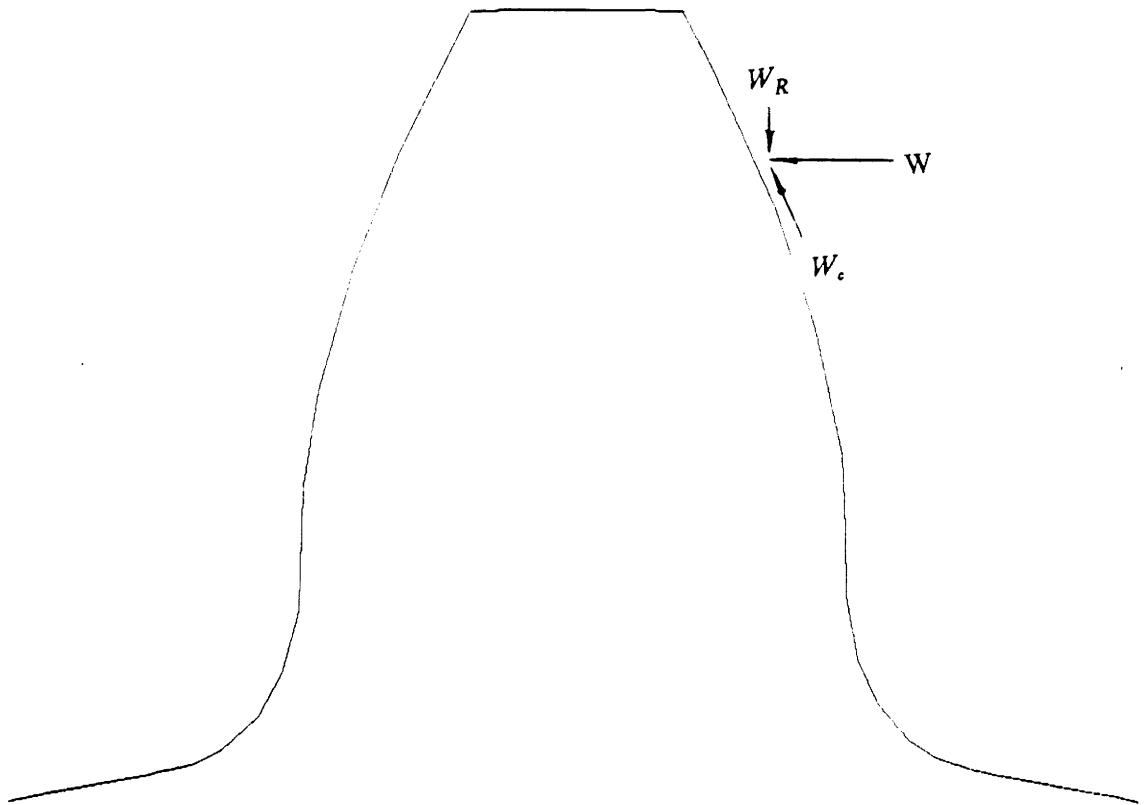


Figure 27. Three forces in the FEM model

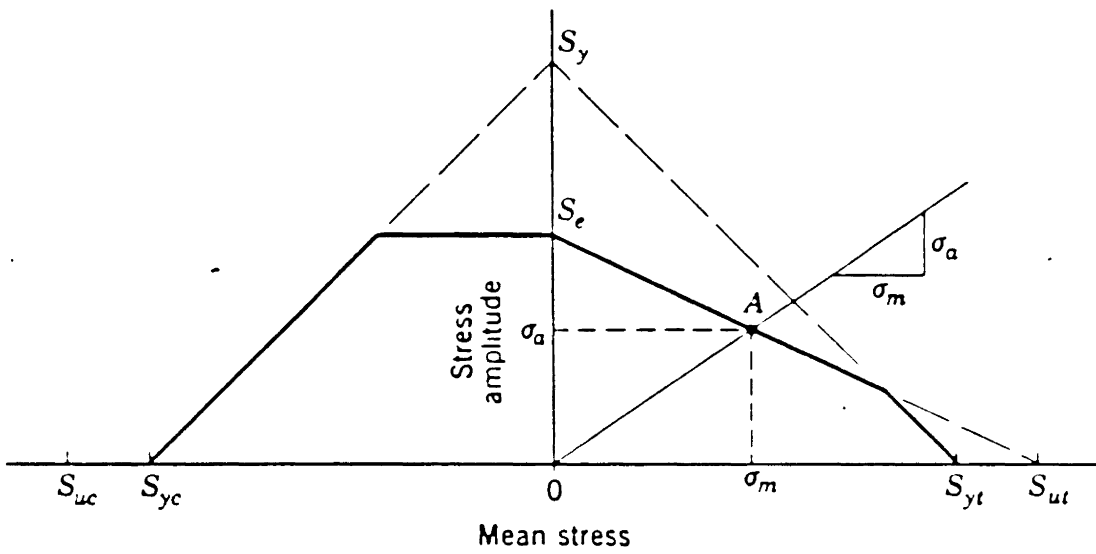


Figure 28. Fatigue diagram

S_y : yield strength

S_u : ultimate strength

S_e : endurance limit

σ_m : mean stress

σ_a : stress amplitude

$$\begin{aligned}\sigma_m &= \sigma_a \\ &= \frac{\sigma_4}{2}\end{aligned}$$

Point A is the limiting values of σ_m and σ_a .

Use of the modified Goodman approach does not use the variation of the tensile stresses. Thus, a more complete method can be used since this information can now be developed. Miner's equation [12] can be used to calculate the combined life cycles N_C for the condition of different levels of stresses in one stress cycle.

$$\frac{\alpha_1}{N_1} + \frac{\alpha_2}{N_2} + \frac{\alpha_3}{N_3} = \frac{1}{N_C}$$

where

$$\alpha_1 = \frac{\alpha - \theta_B}{\alpha - \beta}$$

$$\alpha_2 = \frac{\theta_B - \theta_E}{\alpha - \beta}$$

$$\alpha_3 = \frac{\theta_E - \beta}{\alpha - \beta}$$

N_1 : life cycles for

$$\sigma = \frac{\sigma_1 + \sigma_2}{2}$$

N_2 : life cycles for

$$\sigma = \frac{\sigma_3 + \sigma_4}{2}$$

N_3 : life cycles for

$$\sigma = \sigma_5$$

Larger contact ratios cause helical gears transmit power with less shock loading. Therefore, in modern application, more and more helical gears are used. For further studies, it is recommended that two helical gears in mesh be studied instead of two spur gears in mesh. In the force analysis of spur gears, the forces are assumed to act in a single plane. However, for helical gears, the forces are distributed three-dimensional. It will make the analysis technically more complicated.

Bibliography

- [1] Mabe, H. H., and Reinholtz C. F., Mechanisms and Dynamics of Machinery, Fourth Edition, John Wiley & Sons, 1987.
- [2] Buckingham, E., Analytical Mechanics of Gears, First Edition, McGraw-Hill, 1949
- [3] Lewis, W., Investigation of Strength of Spur Gear Teeth, Proceedings Engineers Club, Philadelphia, Pa. 1983.
- [4] Jalilvand, J., "Stress Concentrations in Undercut Spur Gear Teeth Via the Finite Element Method", Master's Thesis, Virginia Polytechnic Institute and State University, Blacksburg, VA, November 1983.
- [5] General Electric CAE International Inc., IDEAS 2.5, 1982.
- [6] General Electric CAE International SUPERB 6.0 Manual, 1983
- [7] Dolan, T. J., and Broghamer, E. L., A Photoelastic Study of Stresses in Gear Tooth Fillets, University of Illinois, Engineering Experiment Station, Bulletin No. 335, 1942.

- [8] American Gear Manufacturers Association, AGMA Standard for Rating the Strength of Spur Gear Teeth, AGMA 220.02, August 1966.

- [9] Wilcox, L., and Coleman, W., Application of Finite Elements to the Analysis of Gear Tooth Stresses, American Society of Mechanical Engineers, Paper No. 72-PTG-10, 1972.

- [10] Mitchiner, R. G., and Mabie, H. H., The Determination of the Lewis Form Factor and the AGMA Geometry Factor J for External Spur Gear Teeth, Journal of Mechanical Design, Transaction of the ASME, Vol. 104, No. 1, PP.148-158, Jan. 1982.

- [11] Shigley, J. E., and Mitchell, L., D., Mechanical Engineering Design, Fourth Edition, McGraw-Hill, 1983.

- [12] Spotts, M. F., Design of Machine Elements, Fifth Edition

Appendix A. Geometry of The Spur Tooth

A.1 Introduction

In Appendix A, the geometry of a spur tooth is presented. Determination of the position for loading the tooth for the largest principal stress, the stress at the Lewis point and the stresses based on the AGMA standard and Jalilvand method are also explained.

A.2 Tooth profile definition

It was necessary to derive the equations of the trochoid and involute to describe the profile of the tooth. Fig. 29 [4] shows a half tooth indicating its pitch and base circle. From this figure it can be derived that angle AOC (A is a point on involute) is equal to:

$$AOC = \frac{\pi}{2N} + \text{inv}\varphi - \text{inv}\alpha \quad [A.1]$$

where

$$inv\varphi = \tan \varphi - \varphi$$

$$inv\alpha = \tan \alpha - \alpha$$

and

$$R_\alpha = R \frac{\cos \varphi}{\cos \alpha} \quad [A.2]$$

As Fig. 29 shows, the coordinates of point A can be determined as:

$$\begin{aligned} X_A &= R_\alpha \sin(AOC) \\ &= R \frac{\cos \varphi}{\cos \alpha} \sin\left(\frac{\pi}{2N} + inv\varphi - inv\alpha\right) \end{aligned} \quad [A.3]$$

$$\begin{aligned} Y_A &= R_\alpha \cos(AOC) \\ &= R \frac{\cos \varphi}{\cos \alpha} \cos\left(\frac{\pi}{2N} + inv\varphi - inv\alpha\right) \end{aligned} \quad [A.4]$$

The coordinates of points on the trochoid of the tooth have been defined parametrically by Mitchiner and Mabie [10] (Fig. 30) as:

$$\begin{aligned} X_E &= (R - b + r_f) \sin(\beta + \theta) - R\theta \cos(\beta + \theta) \\ &\quad - \frac{r_f}{\sqrt{(b - r_f)^2 + R^2\theta^2}} [R\theta \cos(\beta + \theta) + (b - r_f) \sin(\beta + \theta)] \end{aligned} \quad [A.5]$$

$$\begin{aligned} Y_E &= (R - b + r_f) \cos(\beta + \theta) - R\theta \sin(\beta + \theta) \\ &\quad + \frac{r_f}{\sqrt{(b - r_f)^2 + R^2\theta^2}} [R\theta \sin(\beta + \theta) - (b - r_f) \cos(\beta + \theta)] \end{aligned} \quad [A.6]$$

where

$$\beta = \frac{\pi}{N} - \eta \quad [A.7]$$

$$\eta = \frac{\Delta}{R} \quad [A.8]$$

and

$$\Delta = \frac{\pi}{4P} - (b - r_f) \tan \varphi - \frac{r_f}{\cos \varphi} \quad [A.9]$$

It was also necessary to locate the point of tangency or the point of intersection of the involute tooth flank and the trochoidal tooth root (point I). For this purpose, a computer program has been written, using the Newton-Rhapson method to solve equations A.3, A.4, A.5 and A.6 for α and θ .

Coordinates of the points on the root circle and those on the addendum circle can be determined from Fig 28 as follows:

$$X_R = (R - b) \sin \theta \quad [A.10]$$

$$Y_R = (R - b) \cos \theta \quad [A.11]$$

$$X_D = (R + a) \sin \theta \quad [A.12]$$

$$Y_D = (R + a) \cos \theta \quad [A.13]$$

A program [Appendix B] was written which will calculate the coordinates of points on the root circle using equations A.10 and A.11 with θ ranging from $\frac{\pi}{N}$ to β (see Fig. 29), then the program will calculate the coordinates of points on the trochoid using equations A.5 and A.6 with the parameter θ starting from zero through the point of intersection (see Fig. 30). The program, using equations A.3 and A.4, will determine coordinates of points on the involute from intersection point I until α is equal to γ ,

$$\gamma = \cos^{-1} \left[\frac{R \cos \phi}{R + a} \right] \quad [A.14]$$

Equations A.12 and A.13 can be used to determine the coordinates of points on the addendum circle during the range of

$$\left[\frac{\pi}{2N} + \text{inv} \phi - \text{inv} \gamma \right] \leq \theta \leq 0.0$$

A.3 Loading the tooth for the largest principal stress

AGMA and Jalilvand have calculated the largest stress on the root fillet when a concentrated force is applied on the tooth flank. For the case of load sharing in one gear as shown in Fig. 31 [10], the point U is highest intersection of the line of action and centerline when only one tooth is in engagement.

Mitchiner and Mabie [10] have derived the distance R_c between U and the center of the pinion as:

$$R_{O2} = R_2 + a \quad [A.15]$$

$$\tau = \sin^{-1} \left(\frac{R_2}{R_{O2}} \cos \phi \right) \quad [A.16]$$

$$R_X = \sqrt{Q^2 + R_1^2 - 2QR_1 \sin \phi} \quad [A.17]$$

where

$$Q = \frac{\cos(\tau + \phi)}{\sin \tau} R_2 \quad [A.18]$$

Now

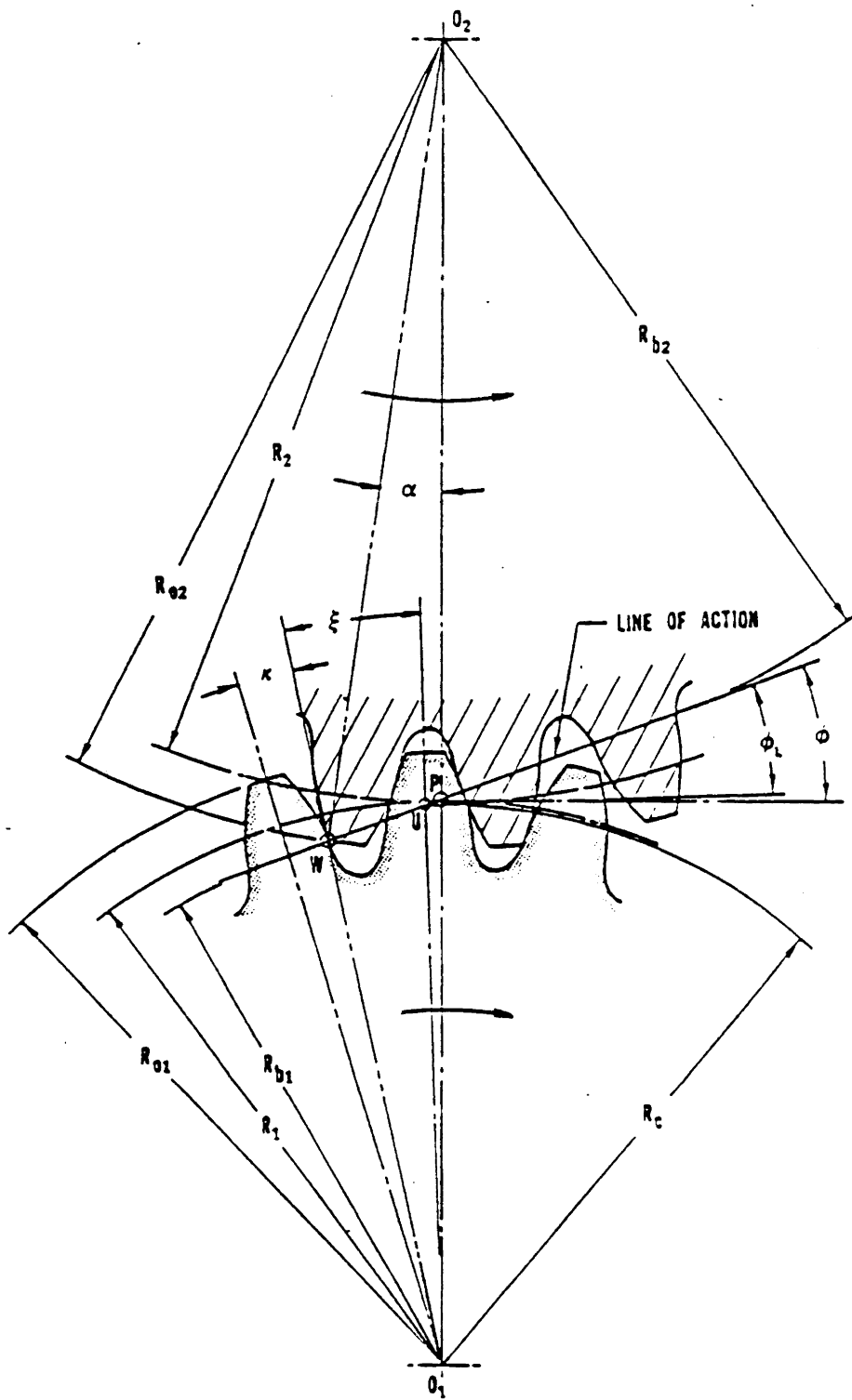


Figure 31. Load at highest point for one tooth contact [5]

$$K = \frac{\pi}{2N} - \text{inv}\left\{\cos^{-1}\left(\frac{R_1 \cos \varphi}{R_\alpha}\right)\right\} + \text{inv}\varphi \quad [A.19]$$

$$\xi = 2\frac{\pi}{N} - K \quad [A.20]$$

$$\zeta = \cos^{-1}\left\{\frac{R_X^2 + R_{O2}^2 - (R_1 + R_2)^2}{2R_X R_{O2}}\right\} - \tau \quad [A.21]$$

then

$$R_C = \frac{R_X \sin(\zeta)}{\sin(\zeta + \xi)} \quad [A.22]$$

φ_L , the angle between the line of action and the horizontal, is given by:

$$\varphi_L = \tan^{-1}\left\{\frac{1 - \left(\frac{R}{R+a} \cos \varphi\right)^2}{\frac{R}{R+a} \cos \varphi}\right\} - \frac{\pi}{2N} - \text{inv}\left\{\tan^{-1}\left[\frac{1 - \left(\frac{R}{R+a} \cos \varphi\right)^2}{\frac{R}{R+a} \cos \varphi}\right]\right\} + \text{inv}\varphi \quad [A.23]$$

A.4 Stress at the Lewis point

For the purpose of computing stress concentration factors, the cantilever beam stress at Lewis point was calculated. The theoretical weakest location is the point of tangency of a parabola inscribed in tooth profile with its apex at point U (Fig. 31) and tangent to the tooth as shown in Fig. 32 [7].

To locate Lewis point, a subroutine based upon the procedure expressed by Mitchiner and Mabie [10] was written. Using Newton-Raphson method and finite differences to approximate derivatives, Lewis point (X_L , Y_L) and R_C were computed numerically.

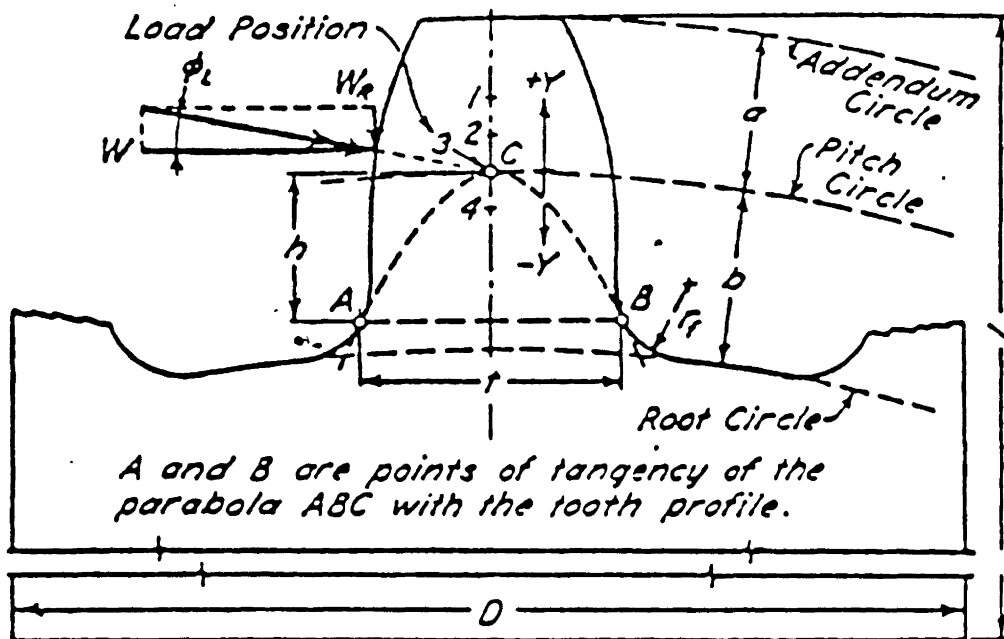


Figure 32. Location of the Lewis point [7]

With the coordinates of point U and Lewis point, the tensile or compressive stress was determined by means of Lewis equation:

$$S_L = \frac{6Wh}{t^2} \quad [A.24]$$

where

$$h = R_C - Y_L \quad [A.25]$$

The direct stress S_R due to compression by applied load was obtained by dividing the radial component of the load, W_R , by the cross-section area of the tooth. This stress was then added algebraically to the stress computed from Lewis equation to give the combined bending and normal stress σ .

$$\begin{aligned} S_R &= \frac{W_R}{t} \\ &= \frac{W \tan \phi_L}{t} \end{aligned} \quad [A.26]$$

$$\begin{aligned} \sigma &= S_L - S_R \\ &= \frac{6Wh}{t^2} - \frac{W \tan \phi_L}{t} \end{aligned} \quad [A.27]$$

A.5 Stresses based on the AGMA standard and Jalilvand fomula

AGMA [8] defines the Lewis form factor Y as:

$$Y = \frac{P}{\frac{\cos \phi_L}{\cos \phi} \left(\frac{1.5}{X_L} - \frac{\tan \phi_L}{t} \right)} \quad [A.28]$$

The geometry factor J is defined as:

$$J = \frac{Y}{K_D m_N} \quad [A.29]$$

Where K_D is the concentration factor defined by Dolan and Broghamer [7]. For a 20° pressure angle, AGMA uses the equation to estimate K_D .

$$K_D = 0.18 + \left(\frac{t}{r_f}\right)^{0.15} \left(\frac{t}{h}\right)^{0.45} \quad [A.30]$$

The m_N may be taken as profile contact ratio m_p . In this condition, load is applied to only one tooth. As such, m_N is considered to be 1.00. Therefore, the bending stress is calculated based on AGMA standard as:

$$\sigma_{AGMA} = W_t \frac{P}{FJ} \quad [A.31]$$

where

W_t : transmitted tangential load in pounds at operating pitch diameter

F: face width of the tooth (unit width was used in this study)

In Jalilvand's [4] work, the concentration factor is defined as:

$$K_J = -1.253234r_f + 0.675457t - 1.772389h + 2.976752 \quad [A.32]$$

And the bending stress at Lewis point based on Jalilvand is:

$$\sigma_{Jal} = K_J \sigma \quad [A.33]$$

Appendix B. Computer Program - TOOTH

```
C
C
C THIS PROGRAM IS TO GENERATE THE GEOMETRY OF THE TEETH
C
C
DIMENSION NOEN(4),JJX(4),X(3000),Y(3000),NEND(4),NST(4),NPTS(9,15)
DIMENSION NM(8)
CHARACTER*10 FINAM
CHARACTER*4 EXT,DAT
CHARACTER*15 FNPNT,FNLIN,FNEDG,FNDAT
REAL N
COMMON/TOOTH/N,P,A,D,RHF,THKNSS,PHI,R
DATA PI/3.1415927/,IYES/1HY/,EXT/'.TTH'/,DAT/'.INF'/
322 TYPE 11
11 FORMAT(' ENTER DIAMETRAL PITCH, ADDENDUM FRACTION,
C DEDENDUM FRACTION',/,
C ' HOB TIP RADIUS, NUMBER OF TEETH ',/)
```

```

ACCEPT *, P,A,D,RHF,N
TYPE 80
80  FORMAT($,' IS THIS TO BE A STANDARD GEAR < Y OR N > ? ' )
ACCEPT 81, IRPLY
81  FORMAT(A1)
TT = PI/(2.*P)
WW = N/(2.*P)
IF(IRPLY.NE.IYES) GO TO 85
R = WW
THKNSS = TT
TYPE 83
83  FORMAT($,' ENTER CUTTING PRESSURE ANGLE IN DEGREES ' )
ACCEPT *, PHIDEG
GO TO 84
85  TYPE 12, WW,TT
12  FORMAT(' ON CUTTING PITCH CIRCLE ENTER',/, ' CUTTING '
1  ' PITCH RADIUS (',F15.9,' FOR STD GEARS)',/,
2  ' CUTTING PRESSURE ANGLE IN DEGREES',/,
3  ' TOOTH THICKNESS (',F15.9,' FOR STD GEARS',//)
ACCEPT *, R,PHIDEG,THKNSS
84  PHI = PHIDEG*PI/180.
TYPE 14, P,A,D,RHF,N,R,PHIDEG,THKNSS
14  FORMAT(' INPUT DATA : ',/,
1  ' PITCH      ',F15.7,/,
2  ' ADD. FRACTION ',F15.7,/,
3  ' DED. FRACTION ',F15.7,/,
*  ' HOB TIP RAD  ',F15.7,/,
4  ' NO. OF TEETH ',F15.7,/,

```

```

5 ' CTG. PITCH R ',F15.7,/,
6 ' CTG. PR. ANG. ',F15.7,/,
7 ' TOOTH THKNSS ',F15.7,////,
8 ' ENTER THE NO OF INTERVALS PER CURVE < 24 MAX - 4 MIN > 'i)
ACCEPT *, XINT
INTERVL = IFIX(XINT + .5)
SPACNG = .01*((A + D)/P)
SPMIN = .95*SPACNG
SPMAX = 1.05*SPACNG
X(1) = 0.
Y(1) = 0.
C
C LOCATE INTERSECTION/TANGENCY POINT
C
CALL INTERSECT(RI,XI,YI,ALPHA,THETA,ITER,0,IER)
C
C
IF(IER.NE.0) TYPE 320
320 FORMAT(' CANNOT LOCATE TROCH/INVOLUTE INTERSECTION')
IF(IER.EQ.99) TYPE 328
328 FORMAT(' LACK OF CONVERGENCE IN 2000 ITERATIONS')
IF(IER.EQ.1) TYPE 329
329 FORMAT(' POINT OF INTERSECTION NOT LOCATED PAUSIBLY')
IF(IER.EQ.1) GO TO 322
IF(IER.EQ.0) TYPE 331, XI,YI,RI,ITER
331 FORMAT(' INTERSECTION POINT LOCATED AT (',F12.8,' ',F12.8,' )',/,
1 ' AT RADIUS OF ',F12.8,/,

```

```

2      ' POINT LOCATED IN ',I5,' ITERATIONS.')
C
C
C LOCATE LEWIS POINT
C
330 CALL POINT(RLEWIS,XLEWIS,YLEWIS,TOUT,ITER,1,IER,RC)
C
      IF(IER.NE.0) TYPE 420
420  FORMAT(' CANNOT LOCATE LEWIS POINT')
      IF(IER.EQ.99) TYPE 428
428  FORMAT(' LACK OF CONVERGENCE IN 2000 ITERATIONS')
      IF(IER.EQ.1) TYPE 429
429  FORMAT(' POINT OF INTERSECTION NOT LOCATED PLAUSIBLY')
      IF(IER.EQ.1) GO TO 322
      IF(IER.EQ.0) TYPE 430, XLEWIS,YLEWIS,RLEWIS,TOUT,ITER,RC
430  FORMAT(' LEWIS POINT LOCATED AT (',F12.8,' ',F12.8,' )',/,
1      ' AT RADIUS OF ',F12.8,' AND THETA OF ',F12.8,/,
2      ' LEWIS POINT LOCATED IN ',I5,' ITERATIONS.',
3      ' RC=',E12.5)
C
C
C ANGLE OF LINE OF ACTION FOR SINGLE TOOTH LOADING.
C
C
      TEMP = ATAN(SQRT(1.-(R*COS(PHI)/(R + A))**2)/(R*COS(PHI)/(R + A)))
      PHIL = TEMP-PI/(2.*N)-XINV(TEMP) + XINV(PHI)
      PHILDEG = PHIL*180./PI

```

```

TYPE *, 'PHIL = ',PHILDEG
C
C
C  STRESS AT LEWIS'
C
C
WLOAD = 1.*COS(PHIL)
HEIGHT = RC-YLEWIS
TYPE *, 'HEIGHT = ',HEIGHT
THICKNS = 2.*XLEWIS
TYPE *, 'THICKNESS = ',THICKNS
STRESS = 6.*WLOAD*HEIGHT/THICKNS**2
SIGMA = STRESS-WLOAD*TAN(PHIL)/THICKNS
C
C  DEVELOP ROOT CIRCLE
C
DELTA = ((PI/P-THKNSS)/2.)-(D/P-RHF/P)*TAN(PHI)-RHF/(P*COS(PHI))
ETA = DELTA/R
BETA = PI/N-ETA
XE = (R-D/P)*SIN(BETA)
YE = (R-D/P)*COS(BETA)
XS = (R-D/P)*SIN(PI/N)
YS = (R-D/P)*COS(PI/N)
XL = SQRT((XS-XE)**2 + (YS-YE)**2)
BETA = PI/N-ATAN(XE/YE)
LL = IFIX(XL/SPACNG)
IF(LL.EQ.0) LL = 1
IF(LL.GT.INTERVL) LL = INTERVL

```

```

DEL = 23./24.*BETA/FLOAT(LL)
TH = PI/N + DEL
DO 120 I = 2,3000
TH = TH-DEL
X(I) = (R-D/P)*SIN(TH)
Y(I) = (R-D/P)*COS(TH)
IF(X(I).LE.XE) GO TO 121
120 CONTINUE
121 X(I) = XE
Y(I) = YE
IDEDTROCH = I
NN = I + 1
C
DEL = .01
TH = -DEL + 1.E-7
C
C TROCHOID
C
SPMINN = SPMIN
SPMAXX = SPMAX
65 NNN = NN
TH = -DEL + 1.E-7
NTROCHPT = 0
DO 60 I = NNN,3000
\ NTROCHPT = NTROCHPT + 1
61 CONTINUE
TH = TH + DEL
C

```

```

CALL TROCH(X(I),Y(I),TH)
XX = X(I)-X(I-1)
YY = Y(I)-Y(I-1)
SP = SQRT(XX*XX + YY*YY)
IF(SP.GE.SPMINN.AND.SP.LE.SPMAXX) GO TO 63
TH = TH-DEL
IF(SP.GT.SPMAXX) DEL = .99*DEL
IF(SP.LT.SPMINN) DEL = 1.01*DEL
GO TO 61
C
63  RM = SQRT(X(I)**2 + Y(I)**2)
    IF(RM.GE.RI.AND.NTROCHPT.LT.INTERVL) GO TO 70
    IF(RM.LT.RI) GO TO 60
    SPMAXX = SPMAXX*1.1
    SPMINN = SPMAXX*.9
    GO TO 65
60  CONTINUE
70  X(I) = XI
    Y(I) = YI
    ITROCHINV = I
    NN = I + 1
    DEL = .01
    ALPHA = ALPHAI
    RO = R + A/P
C
C  INVOLUTE
C
    SPMAXX = SPMAX

```

```

SPMINN = SPMIN
170  NNN = NN
      NINVPT = 0
      ALPHA = ALPHAI-DEL
      DO 10 I = NNN,3000
      NINVPT = NINVPT + 1
161  CONTINUE
      ALPHA = ALPHA + DEL
      CALL INVOL(X(I),Y(I),ALPHA)
      XX = X(I)-X(I-1)
      YY = Y(I)-Y(I-1)
      SP = SQRT(XX*XX + YY*YY)
      IF(SP.GE.SPMINN.AND.SP.LE.SPMAXX) GO TO 163
      ALPHA = ALPHA-DEL
      IF(SP.GT.SPMAXX) DEL = .99*DEL
      IF(SP.LT.SPMINN) DEL = 1.01*DEL
      GO TO 161
C
163  RM = SQRT(X(I)**2 + Y(I)**2)
      IF(RM.GE.RO.AND.NINVPT.LT.INTERVL) GO TO 20
      IF(RM.LT.RO) GO TO 10
      SPMAXX = SPMAXX*1.1
      SPMINN = SPMAXX*.9
      GO TO 170
10  CONTINUE
20  NN = I-1
      IINVADD = I-1

```

```

NNX = NN
C
C   DEVELOP ADDENDUM CIRCLE
C
PHIA = ACOS(R/(R + A/P)*COS(PHI))
TO = (R + A/P)*(THKNSS/(2.*R) + XINV(PHI)-XINV(PHIA))
BETA = TO/(R + A/P)
LL = IFIX(TO/SPACNG)
IF(LL.EQ.0) LL = 1
IF(LL.GT.INTERVL) LL = INTERVL
DEL = 1.001*BETA/FLOAT(LL)
TH = BETA + DEL
DO 270 I = NN,3000
TH = TH-DEL
X(I) = (R + A/P)*SIN(TH)
Y(I) = (R + A/P)*COS(TH)
IF(X(I).LE.0) GO TO 271
270 CONTINUE
271 X(I) = 0.
Y(I) = R + A/P
NN = I
IEND = I
C
C
C   STRESS CONCENTRATION FACTOR
C
DOLANK = .18 + (THICKNS/RHF)**.15*(THICKNS/HEIGHT)**.45
C

```

C

C

TYPE 273

273 FORMAT(' DO YOU WANT A SCREEN DWG OF THE TOOTH',

C ' HALF ? <Y OR N> ', \$)

ACCEPT 81, IRPLY

IF(IRPLY.NE.IYES) GO TO 900

C

C

CALL INITT(1)

CALL BINITT

C CALL DLIMY(0.,RO)

C CALL DLIMX(0.,RO)

X(1)=FLOAT(NN-1)

Y(1)=FLOAT(NN-1)

CALL CHECK(X,Y)

CALL DSPLAY(X,Y)

CALL TINPUT(IOP)

C

C OUTPUT TO SDRC GRAPHICS FILES

C

900 TYPE 901

901 FORMAT(' DO YOU WANT OUTPUT TO SDRC-TYPE FILES <Y OR N> ? ', \$)

ACCEPT 902, IRPLY

902 FORMAT(A1)

IF(IRPLY.NE.IYES) GO TO 1000

TYPE 906

906 FORMAT(' ENTER THE NAME OF THE FILE '

```

C ' TO BE WRITTEN - ', $)
ACCEPT 907, FINAM
907 FORMAT(A)
FNPNT = FINAM//EXT
FNDAT = FINAM//DAT
TYPE 908, FNPNT
908 FORMAT(1X,A,' CONTAINS THE POINT, CIRCLE, SPLINE, LINE DATA')
OPEN(UNIT = 21,NAME = FNPNT,TYPE = 'UNKNOWN')
OPEN(UNIT = 22,NAME = FNDAT,TYPE = 'UNKNOWN')
C
TYPE 1300
1300 FORMAT(' ENTER RADIUS OF HOLE IN BLANK')
ACCEPT *, HRADIUS
TYPE 2000
2000 FORMAT(' ENTER NUMBER OF TEETH IN FE MODEL')
ACCEPT *, XTEETH
LTEETH = IFIX(XTEETH + .5)
LLTH = (LTEETH/2)*2
IF(LLTH.EQ.LTEETH) LTEETH = LTEETH + 1
C
C GENERATE 2ND HALF OF TOOTH IN X AND Y
C
LEND = 2*IEND-3
LL = IEND
DO 2010 I = IEND + 1,LEND
LL = LL-1
X(I) = -X(LL)
2010 Y(I) = Y(LL)

```

```

C
C
C POINT FILE
C
WRITE(21,903)
903 FORMAT(' -1',/, ' 25')
C
IPTNUM = 1
ZETA = 2.*PI/N
XI = FLOAT((LTEETH/2))*ZETA + ZETA
C
C
DO 2100 I = 1, LTEETH
XI = XI - ZETA
DO 2200 J = 2, LEND
IPTNUM = IPTNUM + 1
XNEW = Y(J)*SIN(XI) + X(J)*COS(XI)
YNEW = Y(J)*COS(XI) - X(J)*SIN(XI)
WRITE(21,2210) IPTNUM, XNEW, YNEW
2210 FORMAT(I10,9X,'0',19X,'8',2E13.5,10X,'0.0')
IF (I.NE.1.AND.J.NE.2) GO TO 2200
X6 = 0.0
Y6 = -SQRT(XNEW**2 + YNEW**2)
2200 CONTINUE
2100 CONTINUE
XI = FLOAT((LTEETH/2))*ZETA + PI/N
XNEW = (R-D/P)*SIN(-XI)
YNEW = (R-D/P)*COS(-XI)

```

```

IPTNUM= IPTNUM + 1
WRITE(21,2210) IPTNUM,XNEW,YNEW
WRITE(21,909)
909  FORMAT('  -1')
C
C  SPLINE FILE
C
WRITE(21,1200)
1200 FORMAT('  -1',/, ' 28')
NM(1)= (IDEDTROCH-2) + 1
NM(2)= (ITROCHINV-IDEDTROCH) + 1
NM(3)= (IINVADD-ITROCHINV) + 1
NM(4)= (IEND-IINVADD) + 1
NPTS(1,1)= 2
NPTS(2,1)= IDEDTROCH
NPTS(3,1)= ITROCHINV
NPTS(4,1)= IINVADD
NPTS(5,1)= IEND
NPTS(6,1)= IEND + NM(4)-1
NPTS(7,1)= IEND + NM(4) + NM(3)-2
NPTS(8,1)= IEND + NM(4) + NM(3) + NM(2)-3
NPTS(9,1)= IEND + NM(4) + NM(3) + NM(2) + NM(1)-4
NM(5)= NM(4)
NM(6)= NM(3)
NM(7)= NM(2)
NM(8)= NM(1)
DO 3000 I= 2,15
DO 3001 J= 1,9

```

```

      NPTS(J,I) = NPTS(J,I-1) + 2*IEND-4
3001 CONTINUE
3000 CONTINUE
C
      DO 3010 J = 1, LTEETH
      DO 3020 I = 1, 8
      LABEL = (J-1)*8 + I
      WRITE(21,3030) LABEL, NM(I)
3030 FORMAT(I10,9X,'1',9X,'8',9X,'1',I10)
      WRITE(21,3040) (L, L = NPTS(I,J), NPTS(I+1,J))
3040 FORMAT(8I10)
3020 CONTINUE
3010 CONTINUE
      WRITE(21,909)
C
C   POINT FILE FOR HOLE & LINE OF ACTION
C
      WRITE(21,903)
      XI = FLOAT((LTEETH/2))*ZETA + PI/N
      X1 = 0.
      Y1 = HRADIUS
      X2 = HRADIUS*SIN(XI)
      Y2 = HRADIUS*COS(XI)
      X3 = HRADIUS*SIN(-XI)
      Y3 = HRADIUS*COS(-XI)
      X4 = 0.0
      Y4 = RC
      X5 = 2.0*COS(PHIL)

```

```

Y5 = 2.*SIN(PHIL) + RC
X7 = 0.0
Y7 = -Y1
N1 = NPTS(9,LTEETH) + 1
N2 = N1 + 1
N3 = N2 + 1
N4 = N3 + 1
N5 = N4 + 1
N6 = N5 + 1
N7 = N6 + 1
WRITE(21,2210) N1,X3,Y3
WRITE(21,2210) N2,X1,Y1
WRITE(21,2210) N3,X2,Y2
WRITE(21,2210) N4,X4,Y4
WRITE(21,2210) N5,X5,Y5
WRITE(21,2210) N6,X6,Y6
WRITE(21,2210) N7,X7,Y7
WRITE(21,909)

C
C  CIRCLE FILE FOR HOLE
C
WRITE(21,1400)
1400 FORMAT('  -1',/, ' 27',/,9X,'1',9X,'1',9X,'8',9X,'1')
WRITE(21,1410) N1,N2,N3
1410 FORMAT(3I10)
WRITE(21,1401)
1401 FORMAT(9X,'2',9X,'1',9X,'8',9X,'1')
WRITE(21,1410) N3,N7,N1

```

```

WRITE(21,1402)
1402 FORMAT(9X,'3',9X,'1',9X,'8',9X,'1')
WRITE(21,1411) N6,NPTS(9,LTEETH)
1411 FORMAT(9X,'2',2I10)
WRITE(21,909)
C
C LINE FILE
C
WRITE(21,913)
913 FORMAT(' -1',/, ' 26')
WRITE(21,914) NPTS(9,LTEETH),N1
914 FORMAT(9X,'1',9X,'8',9X,'1',2I10)
WRITE(21,915) N3
915 FORMAT(9X,'2',9X,'8',9X,'1',9X,'2',I10)
WRITE(21,916) N4,N5
916 FORMAT(9X,'3',9X,'8',9X,'1',2I10)
WRITE(21,909)
C
C DATA FILE
C
WRITE(22,930) P,A,D,RHF,N,R,PHIDEG,THKNSS,XLEWIS,YLEWIS,
1 RC,PHILDEG,STRESS,SIGMA,DOLANK,SPACNG
930 FORMAT(' INPUT DATA : ',/,
1 ' PITCH ',F15.8,/,
2 ' ADD. FRACTION ',F15.8,/,
3 ' DED. FRACTION ',F15.8,/,
* ' HOB TIP RAD ',F15.8,/,
4 ' NO. OF TEETH ',F15.8,/,

```

```

5 ' CTG. PITCH R ',F15.8/,
6 ' CTG. PR. ANG. ',F15.8/,
7 ' TOOTH THKNSS ',F15.8/,
9 ' X LEWIS POINT ',F15.8/,
1 ' Y LEWIS POINT ',F15.8/,
2 ' POINT K REDIUS',F15.8/,
3 ' PHI(L)      ',F15.8/,
4 ' LEWIS STRESS ',F15.8/,
5 ' COMBINED STRESS',F15.8/,
6 ' STRESS CONCEN.',F15.8/,
8 ' POINT SPACING ',F15.8,/)

```

1000 CONTINUE

C

C SCALED HARD PLOTTER OUTPUT

C

TYPE 1001

1001 FORMAT(' DO YOU WANT SCALED PLOTTER OUTPUT ? < Y OR N > ', \$)

ACCEPT 81, IRPLY

IF(IRPLY.NE.IYES) GO TO 1005

C

TYPE 1002

1002 FORMAT(' HOW MANY TEETH ARE TO BE DRAWN ? ', \$)

ACCEPT *, NTEETH

TYPE 1003

1003 FORMAT(' WHAT MULTIPLIER (TIMES FULL SIZE) IS TO BE USED ? ', \$)

ACCEPT *, SCALE

TYPE 1004

1004 FORMAT(' DO YOU WANT ADD, DED, PITCH, AND BASE CIRCLES SHOWN ? ',

```

C ' <Y OR N> ', $)
ACCEPT 81, JRPLY
ICIR = 0
IF(JRPLY.EQ.IYES) ICIR = 1
1005 CONTINUE
STOP
END
C
C
FUNCTION XINV(X)
XINV = TAN(X)-X
RETURN
END
C
C
C
SUBROUTINE INTERSECT(RI,X,Y,AOUT,TOUT,ITER,IDBUG,IER)
C
C THIS ROUTINE WILL LOCATE THE POINT OF TANGENCY OR THE POINT
C OF INTERSECTION OF THE INVOLUTE TOOTH FLANK AND THE TROCHOIDAL
C TOOTH ROOT FOR STANDARD OR NON-STANDARD EXTERNAL INVOLUTE
C GEAR TEETH
C
C ARGUMENTS:
C RI RADIUS OF INTERSECTION/TANGENCY POINT
C X,Y COORDINATES OF THE POINT OF INTERSECTION/TANGENCY
C AOUT ALPHA OF THE INVOLUTE @ INTERSECTION
C TOUT THETA OF THE TROCHOID @ INTERSECTION

```

```

C   ITER  ITERATION COUNT TO SOLUTION
C   IDBUG  0 FOR NO OUTPUT OF SUBROUTINE
C         1 FOR OUTPUT AT EACH ITERATION
C   IER   0 FOR PLAUSIBLE OUTPUT
C         1 FOR RI IN AN UNREASONABLE RANGE
C         99 FOR LACK OF CONVERGENCE
C
C SUBROUTINES CALLED:
C   DERIV,INVOL,TROCH
C
C
IMPLICIT REAL*8 (A-H,O-Z)
REAL N
COMMON/TOOTH/N,P,A,D,RHF,THKNSS,PHI,R
REAL*4 X,Y,AOUT,TOUT,XIIS,YIIS,XTIS,YTIS,F1AS,F1TS,F2AS,F2TS,
C   RI,P,D,RHF,THKNSS,PHI,R,A,RO,RMIN
IER = 0
ITER = 0
FACTOR = 1.D0
EPS = 1.D-4
C
C APPROXIMATE ALPHA AND THETA TO BEGIN ITERATION
C AND SET THE HISTORY VARIABLES
C
C ALPHA = .3D0*(1.D0-DEXP(-(DBLE(N)-20.D0)/25.D0))
ALPHA = .70
ALPHAP = ALPHA
THETA = .3D0*(DEXP(-(DBLE(N)-20.D0)/45.D0))

```

```

    THETAP = THETA
C
C   BEGIN LOOP
C
I   CONTINUE
C
C   THIS LOOP LOCATES THE POINT OF TANGENCY OR INTERSECTION
C   BETWEEN THE INVOLUTE AND THE TROCHOID
C
    ITER = ITER + 1
C
C   TEST ITERATION COUNTER FOR LACK OF CONVERGENCE
C
    IF(ITER.GT.2000) GO TO 900
C
C   SET THE FACTORS TO DAMPEN OSCILLATIONS
C
    IF(ITER.GE.10) FACTOR = .10D0
    IF(ITER.GE.50) FACTOR = .01D0
    IF(ITER.GE.200) FACTOR = .001D0
C
C   GET THE DERIVATIVES OF XI-XT (F1) AND YI-YT (F2)
C   SINGLE PRECISION
C
    CALL DERIV(SNGL(ALPHA),SNGL(THETA),F1AS,F1TS,F2AS,F2TS)
    F1A = DBLE(F1AS)
    F1T = DBLE(F1TS)
    F2A = DBLE(F2AS)

```

```

F2T = DBLE(F2TS)
C
C   FORM THE JACOBIAN
C
DJAC = F1A * F2T - F2A * F1T
C
C   GET THE CURRENT LOCATIONS ON THE TROCHOID AND INVOLUTE
C
CALL INVOL(XI1S, YI1S, SNGL(ALPHA))
CALL TROCH(XT1S, YT1S, SNGL(THETA))
XI1 = DBLE(XI1S)
YI1 = DBLE(YI1S)
XT1 = DBLE(XT1S)
YT1 = DBLE(YT1S)
DTEMP1 = (YI1 - YT1) * F1T - (XI1 - XT1) * F2T
DTEMP2 = (XI1 - XT1) * F2A - (YI1 - YT1) * F1A
C
C   COMPUTE THE NEWTON-RHAPSON CORRECTIONS
C
DELA = DTEMP1 / DJAC * FACTOR
DELTH = DTEMP2 / DJAC * FACTOR
ALPHA = ALPHA + DELA
THETA = THETA + DELTH
C
C   COMPUTE ERRORS AND COMPARE WITH ERROR CRITERION
C
EPSA = ABS((ALPHA - ALPHAP) / ALPHA)

```

```

        EPST = ABS((THETA-THETAP)/THETA)
C
C   IF BOTH ERRORS SMALL THEN EXIT
C
        IF(EPST.LT.EPS.AND.EPSA.LT.EPS) GO TO 3
C
C   IF DEBUG SWITCH .NE. 0 WRITE ITERATION RESULTS
C
        IF(IDBUG.NE.0) TYPE 2, ITER, ALPHA,THETA
2   FORMAT(' INTERSECT *** ITER =',I5,' ALPHA = ',D15.8,' THETA = ',
C   D15.8)
        ALPHAP = ALPHA
        THETAP = THETA
C
C   DON'T LET ALPHA OR THETA GO NEGATIVE
C
        IF(ALPHA.LT.0.) ALPHA = 1.D-10
        IF(THETA.LT.0.) THETA = 1.D-10
C
C   START LOOP AGAIN
C
        GO TO 1
C
C   EXIT LOOP
C
3   ALPHAS = SNGL(ALPHA)
        CALL INVOL(X,Y,ALPHAS)
        AOUT = SNGL(ALPHA)

```

```

TOUT = SNGL(THETA)
RI = SQRT(X*X + Y*Y)
RO = R + A/P
RMIN = R - D/P
IER = 1
IF(RI.GE.RMIN.AND.RI.LE.RO) IER = 0
RETURN

C
C  LOOP FOR CONVERGENCE FAILURE
C
900  IER = 99
    RETURN
    END

C
C
SUBROUTINE TROCH(XTR,YTR,TH)
C
C  COMPUTE THE LOCATION OF A POINT ON THE TROCHOID (XTR,YTR)
C  GIVEN THE PARAMETER TH (THETA)
C
REAL N
COMMON/TOOTH/N,P,A,D,RHF,THKNSS,PHI,R
C
C  TROCHOID
C
DELTA = ((PI/P-THKNSS)/2.)-(D/P-RHF/P)*TAN(PHI)-RHF/(P*COS(PHI))
ETA = DELTA/R
BETA = PI/N-ETA

```

```

XTR = -TH*R*COS(BETA + TH) + (R-D*P**(-1) + P**(-1)*RHF)*
CSIN(BETA + TH)-P**(-1)*RHF*(TH**(-1)*R**(-1)*P**(-1)*(
CD-RHF)*(TH**(-2)*R**(-2)*P**(-2)*(D-RHF)**2 + 1.)**(-.5)*
CSIN(BETA + TH) + (TH**(-2)*R**(-2)*P**(-2)*(D-RHF)**2
C + 1.)**(-.5)*COS(BETA + TH))
YTR = TH*R*SIN(BETA + TH) + (R-D*P**(-1) + P**(-1)*RHF)*
CCOS(BETA + TH) + P**(-1)*RHF*(-TH**(-1)*R**(-1)*P**(-1
C)*(D-RHF)*(TH**(-2)*R**(-2)*P**(-2)*(D-RHF)**2 + 1.)**(-.5
C)*COS(BETA + TH) + (TH**(-2)*R**(-2)*P**(-2)*(D-RHF)
C**2 + 1.)**(-.5)*SIN(BETA + TH))
RETURN
END
C
SUBROUTINE INVOL(XINV,YINV,ALPHA)
C
C COMPUTE THE LOCATION OF A POINT ON THE INVOLUTE (XINV,YINV)
C GIVEN THE PARAMETER ALPHA
C
REAL N
COMMON/TOOTH/N,P,A,D,RHF,THKNSS,PHI,R
C
C INVOLUTE
C
XINV = R*COS(PHI)/COS(ALPHA)*SIN(((THKNSS/2.)/R)
C + TAN(PHI)-PHI-TAN(ALPHA) + ALPHA)
YINV = R*COS(PHI)/COS(ALPHA)*COS(((THKNSS/2.)/R)
C + TAN(PHI)-PHI-TAN(ALPHA) + ALPHA)
RETURN

```

```

END
C
SUBROUTINE DERIV(ALPHA,THETA,F1A,F1T,F2A,F2T)
C
C   FORM F1 AS XINV-XTROCH
C   F2 AS YINV-YTROCH
C   TAKE DERIVATIVES W/R ALPHA -- F1A & F2A
C   THETA -- F1T & F2T
C
REAL N
COMMON/TOOTH/N,P,A,D,RHF,THKNSS,PHI,R
ALDEL = ALPHA + .001
THDEL = THETA + .001
CALL INVOL(XI1,YI1,ALPHA)
CALL INVOL(XI2,YI2,ALDEL)
CALL TROCH(XT1,YT1,THETA)
CALL TROCH(XT2,YT2,THDEL)
F1A = (XI2-XI1)*1000.
F1T = -(XT2-XT1)*1000.
F2A = (YI2-YI1)*1000.
F2T = -(YT2-YT1)*1000.
RETURN
END
C
C
C
SUBROUTINE POINT(RI,X,Y,TOUT,ITER,IDBUG,IER,RC)
C

```

```

C THIS ROUTINE WILL LOCATE THE POINT OF HIGHEST TENSILE STRESS
C ON THE ROOT FOR STANDARD OR NON-STANDARD EXTERNAL INVOLUTE
C GEAR TEETH
C
C ARGUMENTS:
C RI RADIUS OF POINT
C X,Y COORDINATES OF THE POINT
C TOUT THETA OF THE TROCHOID @ POINT
C ITER ITERATION COUNT TO SOLUTION
C IDBUG 0 FOR NO OUTPUT OF SUBROUTINE
C 1 FOR OUTPUT AT EACH ITERATION
C IER 0 FOR PLAUSIBLE OUTPUT
C 1 FOR RI IN AN UNREASONABLE RANGE
C 99 FOR LACK OF CONVERGENCE
C RC RADIUS OF K POINT FOR SINGLE-TOOTH LOADING
C
C SUBROUTINES CALLED:
C DERIV,INVOL,TROCH
C
C
IMPLICIT REAL*8 (A-H,O-Z)
REAL N
COMMON/TOOTH/N,P,A,D,RHF,THKNSS,PHI,R
REAL*4 X,Y,TOUT,RI,P,D,RHF,THKNSS,PHI,R,A,RO,RMIN
IER = 0
ITER = 0
DEL = .002
FACTOR = 1.D0

```

```

EPS = 1.D-4
C
C APPROXIMATE THETA TO BEGIN ITERATION
C AND SET THE HISTORY VARIABLE
C
THETA = .2D0*(DEXP(-(DBLE(N)/40.D0))) + .1D-8
THETAP = THETA
C
C BEGIN LOOP
C
1 CONTINUE
C
C THIS LOOP LOCATES THE POINT OF TANGENCY OR INTERSECTION
C BETWEEN THE INVOLUTE AND THE TROCHOID
C
ITER = ITER + 1
C
C TEST ITERATION COUNTER FOR LACK OF CONVERGENCE
C
IF(ITER.GT.2000) GO TO 900
C
C SET THE FACTORS TO DAMPEN OSCILLATIONS
C
IF(ITER.GE.10) FACTOR = .10D0
IF(ITER.GE.50) FACTOR = .01D0
IF(ITER.GE.200) FACTOR = .001D0
C
C GET THE DERIVATIVE

```

```

C   SINGLE PRECISION
C
CALL DERIV2(THETA,FTHETA,FPRIME,RC)
THETAP = THETA
THETA = THETA-FTHETA/FPRIME
C
C   COMPUTE ERROR AND COMPARE WITH ERROR CRITERION
C
EPST = ABS((THETA-THETAP)/THETA)
C
C   IF ERROR SMALL THEN EXIT
C
IF(EPST.LT.EPS) GO TO 3
C
C   IF DEBUG SWITCH .NE. 0 WRITE ITERATION RESULTS
C
IF(IDBUG.NE.0) TYPE 2, ITER, THETA
2  FORMAT(' POINT *** ITER = ',I5, ' THETA = ',D15.8)
C
C   DON'T LET THETA GO NEGATIVE
C
IF(THETA.LT.0.) THETA = 1.D-10
C
C   START LOOP AGAIN
C
GO TO 1
C
C   EXIT LOOP

```

```

C
3  CONTINUE
   THETAS = SNGL(THETA)
   CALL TROCH(X,Y,THETAS)
   TOUT = THETAS
   RI = SQRT(X*X + Y*Y)
   RO = R + A/P
   RMIN = R - D/P
   IER = 1
   IF(RI.GE.RMIN.AND.RI.LE.RO) IER = 0
   RETURN

C
C  LOOP FOR CONVERGENCE FAILURE
C
900  IER = 99
     RETURN
     END

C
   SUBROUTINE DERIV2(THETA,FTHETA,FPRIME,RC)

C
C
C  RC  RADIUS OF POINT K
C
C
   REAL K,N,MJE,MJE2
   COMMON/TOOTH/N,P,A,D,RHF,THKNSS,PHI,R
   PI = 3.1415927
   DEL = .01

```

```

THDEL = THETA + DEL
DELTA = ((PI/P-THKNSS)/2.)-(D/P-RHF/P)*TAN(PHI)-RHF/(P*COS(PHI))
ETA = DELTA/R
BETA = PI/N-ETA
MJE = -(1. + (D-RHF)/(R*THETA))*TAN(BETA + THETA))/
* ((D-RHF)/(R*THETA)-TAN(BETA + THETA))
MJE2 = -(1. + (D-RHF)/(R*THDEL))*TAN(BETA + THDEL))/
* ((D-RHF)/(R*THDEL)-TAN(BETA + THDEL))
R1 = R
R2 = R1*1.
RO2 = R2 + A
TAU = ASIN(R2*COS(PHI)/RO2)
Q = COS(TAU + PHI)*R2/SIN(TAU)
RX = SQRT(Q**2 + R1**2 - 2.*Q*R1*SIN(PHI))
TEMP = ACOS(R1*COS(PHI)/RX)
K = PI/(2.*N)-XINV(TEMP) + XINV(PHI)
PSI = (2.*PI/N)-K
ETHA = ACOS((RX**2 + RO2**2 - ((R1 + R2)**2))/(2.*RX*RO2))-TAU
RC = RX*SIN(ETHA)/SIN(ETHA + PSI)
CALL TROCH(XT,YT,THETA)
CALL TROCH(XT2,YT2,THDEL)
FTHETA = MJE + 2.*(RC-YT)/XT
FTHETA2 = MJE2 + 2.*(RC-YT2)/XT2
FPRIME = (FTHETA2-FTHETA)/DEL
RETURN
END

```

Appendix C. Computer Program - MESH

```
C
C
C THIS PROGRAM IS TO GENERATE THE GEOMETRY OF MESHED GEAR
C
C
C
DIMENSION XXDP(1000),YYDP(1000),XXGDP(1000),YYGDP(1000),JS(8),
&IS(8)
CHARACTER*4 EXT, EXT1, EXT2
CALL ASRE(AA,AR)
CALL POINT(INP,IGNP,XXDP,YYDP,XXGDP,YYGDP,RN1,RN2,P,PHII)
WRITE (*,*) 'INPUT THE NAME OF THE FILE FOR THE PINION'
READ(*,300)EXT
300 FORMAT (A4)
WRITE (*,*) 'INPUT THE NAME OF THE FILE FOR THE MATING GEAR'
READ(*,310)EXT1
310 FORMAT (A4)
WRITE (*,*) 'INPUT THE NAME OF THE NEW FILE'
```

```

    READ(*,320)EXT2
320  FORMAT (A4)
    OPEN(UNIT = 1,FILE = EXT,STATUS = 'OLD')
    OPEN(UNIT = 2,FILE = EXT1,STATUS = 'OLD')
    OPEN(UNIT = 3,FILE = EXT2,STATUS = 'NEW')
C
C  READ DATA FROM DATA FILE FOR THE PINION
C  AND THEN WRITE INTO NEW DATA FILE
C
    READ(1,375)I1
375  FORMAT(I6)
    WRITE(3,375)I1
    READ(1,380)I2
380  FORMAT(I6)
    WRITE(3,380)I2
    ICNP = 1
390  READ(1,400)NCPT,NCCOOR,NCCOL,XCP,YCP,ZCP
400  FORMAT(2I10,10X,I10,3E13.5)
    IF(NCPT.EQ.-1) GO TO 410
    WRITE(3,400)NCPT,NCCOOR,NCCOL,XXDP(ICNP),YYDP(ICNP),ZCP
    ICNP = ICNP + 1
    GO TO 390
410  WRITE(3,*) ' -1'
    READ(1,420)IC3
420  FORMAT(I6)
    WRITE(3,420)IC3
    READ(1,430)IC4
430  FORMAT(I6)

```

```

WRITE(3,430)IC4
INS = 1
435 READ(1,440)NCSP,NCSD,NCSC,NCSL,NCPS
440 FORMAT(5I10)
IF (NCSP.EQ.-1) GO TO 460
WRITE(3,440)NCSP,NCSD,NCSC,NCSL,NCPS
READ (1,445)(JS(K),K = 1,8)
445 FORMAT(8I10)
WRITE (3,445)(JS(K),K = 1,8)
KN = NCPS-8
READ (1,450)(IS(KK),KK = 1,KN)
450 FORMAT(5I10)
WRITE (3,450)(IS(KK),KK = 1,KN)
INS = INS + 1
GO TO 435
460 INS = INS-1
WRITE(3,*) ' -1'
READ(1,470) IC5
470 FORMAT(I6)
WRITE(3,470) IC5
READ(1,475) IC6
475 FORMAT(I6)
WRITE(3,475) IC6
480 READ(1,490)NCPT,NCCOOR,NCCOL,XCP,YCP,ZCP
490 FORMAT(2I10,10X,I10,3E13.5)
IF(NCPT.EQ.-1) GO TO 500
WRITE(3,490)NCPT,NCCOOR,NCCOL,XXDP(ICNP),YYDP(ICNP),ZCP
ICNP = ICNP + 1

```

```

GO TO 480
500 WRITE(3,*)' -1'
    READ(1,520) IC7
520 FORMAT(I6)
    WRITE(3,520) IC7
    READ(1,530) IC8
530 FORMAT(I6)
    WRITE(3,530) IC8
540 READ(1,550)NCA,NCAD,NCAC,NCAL
    IF (NCA.EQ.-1) GO TO 570
550 FORMAT(4I10)
    WRITE(3,550)NCA,NCAD,NCAC,NCAL
    READ(1,560)JA1,JA2,JA3
    WRITE(3,560)JA1,JA2,JA3
560 FORMAT(3I10)
    GO TO 540
570 WRITE(3,*)' -1'
    READ(1,580) IC9
580 FORMAT(I6)
    WRITE(3,580) IC9
    READ(1,590) IC10
590 FORMAT(I6)
    WRITE(3,590) IC10
    READ(1,600)NCL,NCLC,NCLS,NC1,NC2
    WRITE(3,600)NCL,NCLC,NCLS,NC1,NC2
600 FORMAT(5I10)
    READ(1,600)NCL,NCLC,NCLS,NC1,NC2

```

```

WRITE(3,600)NCL,NCLC,NCLS,NC1,NC2
610 WRITE(3,*)' -1'
    READ(2,620)I1
620 FORMAT(I6)
    WRITE(3,620)I1
C
C READ DATA FROM DATA FILE FOR THE GEAR
C AND THEN WRITE INTO NEW DATA FILE
C
    READ(2,630)I2
630 FORMAT(I6)
    WRITE(3,630)I2
    ICNP = 1
640 READ(2,650)NCPT,NCCOOR,NCCOL,XCP,YCP,ZCP
650 FORMAT(2I10,10X,I10,3E13.5)
    IF(NCPT.EQ.-1) GO TO 660
    NCPT = NCPT + INP
    WRITE(3,650)NCPT,NCCOOR,NCCOL,XXGDP(ICNP),YYGDP(ICNP),ZCP
    ICNP = ICNP + 1
    GO TO 640
660 WRITE(3,*)' -1'
    READ(2,670)IC3
670 FORMAT(I6)
    WRITE(3,670)IC3
    READ(2,680)IC4
680 FORMAT(I6)

```

```

WRITE(3,680)IC4
690 READ(2,700)NCSP,NCSD,NCSC,NC SL,NCPS
700 FORMAT(5I10)
IF (NCSP.EQ.-1) GO TO 730
NCSP = NCSP + INS
WRITE(3,700)NCSP,NCSD,NCSC,NC SL,NCPS
READ (2,710)(JS(K),K = 1,8)
710 FORMAT(8I10)
DO 715 IK = 1,8
JS(IK) = JS(IK) + INP
715 CONTINUE
WRITE (3,710)(JS(K),K = 1,8)
KN = NCPS-8
READ (2,720)(IS(KK),KK = 1,KN)
720 FORMAT(5I10)
DO 725 IKK = 1,KN
IS(IKK) = IS(IKK) + INP
725 CONTINUE
WRITE (3,720)(IS(KK),KK = 1,KN)
GO TO 690
730 WRITE(3,*) -1'
READ(2,740) IC5
740 FORMAT(I6)
WRITE(3,740) IC5
READ(2,750) IC6
750 FORMAT(I6)

```

```

WRITE(3,750) IC6
760 READ(2,770)NCPT,NCCOOR,NCCOL,XCP,YCP,ZCP
770 FORMAT(2I10,10X,I10,3E13.5)
IF(NCPT.EQ.-1) GO TO 780
NCPT = NCPT + INP
WRITE(3,490)NCPT,NCCOOR,NCCOL,XXGDP(ICNP),YYGDP(ICNP),ZCP
ICNP = ICNP + 1
GO TO 760
780 WRITE(3,*)' -1'
READ(2,790) IC7
790 FORMAT(I6)
WRITE(3,790) IC7
READ(2,800) IC8
800 FORMAT(I6)
WRITE(3,800) IC8
810 READ(2,820)NCA,NCAD,NCAC,NCAL
IF (NCA.EQ.-1) GO TO 840
820 FORMAT(4I10)
NCA = NCA + 3
WRITE(3,820)NCA,NCAD,NCAC,NCAL
READ(2,830)JA1,JA2,JA3
JA1 = JA1 + INP
JA2 = JA2 + INP
JA3 = JA3 + INP
WRITE(3,830)JA1,JA2,JA3
830 FORMAT(3I10)
GO TO 810
840 WRITE(3,*)' -1'

```

```

      READ(2,850) IC9
850  FORMAT(I6)
      WRITE(3,850) IC9
      READ(2,860) IC10
860  FORMAT(I6)
      WRITE(3,860) IC10
      READ(2,880)NCL,NCLC,NCLS,NC1,NC2
      NCL = NCL + 2
      NC1 = NC1 + INP
      NC2 = NC2 + INP
      WRITE(3,880)NCL,NCLC,NCLS,NC1,NC2
880  FORMAT(5I10)
      READ(2,880)NCL,NCLC,NCLS,NC1,NC2
      NCL = NCL + 2
      NC1 = NC1 + INP
      NC2 = NC2 + INP
      WRITE(3,880)NCL,NCLC,NCLS,NC1,NC2
      WRITE(3,*)' -1'
      WRITE(3,*)' -1'
      WRITE(3,*)' 25'
      NCPT1 = INP + IGNP + 2
      NCPT2 = INP + IGNP + 3
      NCC = 0
      NCOL = 8
      PI = 4.*ATAN(1.)
      XX1 = RN2*P/2.
      YY1 = RN1*P/2. + XX1*TAN(PHII*PI/180.)
      XX2 = -RN2*P/2.

```

```

YY2 = RN1*P/2.-XX1*TAN(PHII*PI/180.)
Z = 0.
WRITE(3,490)NCPT1,NCC,NCOL,XX1,YY1,Z
WRITE(3,490)NCPT2,NCC,NCOL,XX2,YY2,Z
WRITE(3,*)' -1'
WRITE(3,*)' -1'
WRITE(3,*)' 26'
NCL1 = 5
NCL2 = 6
NCLS = 1
WRITE(3,880)NCL1,NCOL,NCLS,NCPT1,NCPT2
WRITE(3,*)' -1'
END

```

C

C THIS SUBROUTINE IS TO READ THE COORDINATES OF THE POINTS ON
C THE PINION AND THE GEAR AND CALCULATE THE NEW POSITIONS
C FOR THE POINTS. WHEN THE PINION IS ROTATED SOME ANGLE,
C THIS SUBROUTINE WILL RECALCULATE THE COORDINATES FOR THE POINTS
C ON THE PINION AND THE GEAR.

C

```

SUBROUTINE POINT(INP,IGNP,XXDP,YYDP,XXGDP,YYGDP,RN1,RN2,P,PHII)
DIMENSION XDP(1000),YDP(1000),XGDPP(1000),YGDPP(1000),
$XGDP(1000),YGDP(1000),XXDP(1000),YYDP(1000),XXGDP(1000),
&YYGDP(1000)
CHARACTER*4 EXT, EXT1
WRITE(*,*)' ENTER THE NAME OF THE FILE FOR THE PINION'
READ(*,5)EXT

```

5 FORMAT (A4)

```

OPEN(UNIT = 7,FILE = EXT,STATUS = 'OLD')
C
C READ THE COORDINATES OF THE POINTS ON THE PINION
C
READ(7,10)I1
10 FORMAT(I6)
READ(7,20)I2
20 FORMAT(I6)
INP = 1
25 READ(7,30)NPT,NCOOR,NCOL,XDP(INP),YDP(INP)
30 FORMAT(2I10,10X,I10,2E13.5)
IF(NPT.EQ.-1) GO TO 40
INP = INP + 1
GO TO 25
40 READ(7,50)I3
50 FORMAT(I6)
READ(7,60)I4
60 FORMAT(I6)
65 READ(7,70)NSP
70 FORMAT(I10)
IF(NSP.EQ.-1) GO TO 80
GO TO 65
80 READ(7,90)I5
90 FORMAT(I6)
READ(7,100) I6
100 FORMAT(I6)
105 READ(7,110)NPT,NCOOR,NCOL,XDP(INP),YDP(INP)
110 FORMAT(2I10,10X,I10,2E13.5)

```

```

IF(NPT.EQ.-1) GO TO 120
INP = INP + 1
GO TO 105
120 INP = INP - 1
WRITE(*,*) 'ENTER THE NAME OF THE FILE FOR THE MATING GEAR'
READ(*,160)EXT1
160 FORMAT (A4)
OPEN(UNIT = 3,FILE = EXT1,STATUS = 'OLD')
C
C READ THE COORDINATES OF THE POINTS ON THE GEAR
C
READ(3,170)IG1
170 FORMAT(I6)
READ(3,180)IG2
180 FORMAT(I6)
IGNP = 1
190 READ(3,200)NGPT,NGCOOR,NGCOL,XGDPP(IGNP),YGDPP(IGNP)
200 FORMAT(2I10,10X,I10,2E13.5)
IF(NGPT.EQ.-1) GO TO 210
IGNP = IGNP + 1
GO TO 190
210 READ(3,220)IG3
220 FORMAT(I6)
READ(3,230)IG4
230 FORMAT(I6)
240 READ(3,250)NGSP
250 FORMAT(I10)
IF(NGSP.EQ.-1) GO TO 260

```

```

GO TO 240
260 READ(3,270)IG5
270 FORMAT(I6)
    READ(3,280) IG6
280 FORMAT(I6)
290 READ(3,300)NGPT,NGCOOR,NGCOL,XGDPP(IGNP),YGDPP(IGNP)
300 FORMAT(2I10,10X,I10,2E13.5)
    IF(NGPT.EQ.-1) GO TO 310
    IGNP = IGNP + 1
    GO TO 290
310 IGNP = IGNP-1
    WRITE (*,*) ' INPUT N1, N2, P,PHI'
    READ (*,*) RN1,RN2,P,PHI
C
C  CALCAULATE THE NEW COORDINATES OF THE POINTS ON THE GAER
C  TO MESH WITH THE PINION
C
    YY=(RN1 + RN2)/(2.*P)
    TH= 180./RN2
    THETA = 180. + TH
    THET = THETA*ATAN(1.0)/45.
    IGNPM = IGNP-2
    DO 350 II = 1,IGNPM
    XTMP = XGDPP(II)
    YTMP = YGDPP(II)
    R = SQRT(XTMP**2 + YTMP**2)
    ALPH = ACOS(XTMP/R)
    BETA = ALPH + THET

```

```

XGDP(II) = R * COS(BETA)
YGDP(II) = R * SIN(BETA) + YY
350 CONTINUE
THTH = TH * ATAN(1.) / 45.
XGDP(IGNP-1) = YGDPP(IGNP-1) * SIN(THTH)
YGDP(IGNP-1) = -YGDPP(IGNP-1) * COS(THTH) + YY
XGDP(IGNP) = YGDPP(IGNP) * SIN(THTH)
YGDP(IGNP) = -YGDPP(IGNP) * COS(THTH) + YY
WRITE (*,*) 'INPUT ANGLE OF ROTATION IN DEGREE'
READ (*,*) RTHETA
IF(RTHETA.EQ.0.) GO TO 500
C
C CALCULATE THE NEW COORDINATES OF THE POINTS ON THE PINION
C AFTER THE PINION IS ROTATED SOME ANGLE
C
PI = 4. * ATAN(1.)
RGTH = RTHETA * RN1 / RN2
INPM = INP - 2
DO 360 IR = 1, INPM
RR = SQRT((XDP(IR)**2 + YDP(IR)**2))
RALPH = ACOS(XDP(IR) / RR)
RBETA = RALPH + RTHETA * PI / 180.
XXDP(IR) = RR * COS(RBETA)
YYDP(IR) = RR * SIN(RBETA)
360 CONTINUE
XXDP(INP-1) = -YDP(INP-1) * SIN(RTHETA * PI / 180.)
YYDP(INP-1) = YDP(INP-1) * COS(RTHETA * PI / 180.)
XXDP(INP) = -YDP(INP) * SIN(RTHETA * PI / 180.)

```

```

YYDP(INP) = YDP(INP)*COS(RTHETA*PI/180.)
C
C  CALCULATE THE NEW COORDINATES OF THE POINTS ON THE GEAR
C  AFTER THE PINION IS ROTATED SOME ANGLE
C
DO 370 IGR = 1,IGNPM
TY1 = YGDP(IGR)-YY
RRG = SQRT((XGDP(IGR)**2 + TY1**2))
RGALPH = ACOS(XGDP(IGR)/RRG)
RGBETA = RGALPH + RGTH*PI/180.
XXGDP(IGR) = RRG*COS(RGBETA)
YYGDP(IGR) = -RRG*SIN(RGBETA) + YY
370 CONTINUE
TYA = YGDP(IGNP-1)-YY
TYB = YGDP(IGNP)-YY
RRGA = SQRT((XGDP(IGNP-1)**2 + TYA**2))
RRGB = SQRT((XGDP(IGNP)**2 + TYB**2))
RGALPH = ACOS(TYA/RRGA)
RGBETA = RGALPH-RGTH*PI/180.
XXGDP(IGNP-1) = -RRGA*SIN(RGBETA)
YYGDP(IGNP-1) = RRGGA*COS(RGBETA) + YY
XXGDP(IGNP) = -RRGB*SIN(RGBETA)
YYGDP(IGNP) = RRGB*COS(RGBETA) + YY
GO TO 600
500 DO 510 KK = 1,INP
XXDP(KK) = XDP(KK)
YYDP(KK) = YDP(KK)
510 CONTINUE

```

```

DO 520 KKK = 1,IGNP
XXGDP(KKK) = XGDP(KKK)
YYGDP(KKK) = YGDP(KKK)
520 CONTINUE
600 CLOSE(UNIT = 7)
CLOSE(UNIT = 3)
RETURN
END

C
C THIS SUBROUTINE IS TO CALCULATE THE APPROACH ANGLE, RECESS ANGLE
C , CONTACT RATIO, THE ANGLE FOR THE BEGINNING OF ONE PAIR OF TEETH
C IN CONTACT AND THE ANGLE FOR THE END OF ONE PAIR OF TEETH IN
C CONTACT
C
SUBROUTINE ASRE(AA,AR)
WRITE (*,*) 'INPUT N1, N2, P, ADD., PHI ( IN DEGREE )'
READ (*,*) RN1,RN2,P,A,PHID
PI = 4.*ATAN(1.)
PHI = PHID*PI/180.
R1 = RN1/(2.*P)
R2 = RN2/(2.*P)
RB1 = R1*COS(PHI)
RB2 = R2*COS(PHI)
RO1 = R1 + A
RO2 = R2 + A
AP = SQRT(RO1**2-RB1**2)-R1*SIN(PHI)
POA = ACOS((R1**2 + RO1**2-AP**2)/(2.*R1*RO1))
PHIO1 = ACOS(RB1/RO1)

```

```

T1 = PI*R1/RN1
TO1 = T1/(2.*R1) + TAN(PHI)-PHI-TAN(PHIO1) + PHIO1
ARR = POA-TO1
BP = SQRT(RO2**2-RB2**2)-R2*SIN(PHI)
POB = ACOS((R2**2 + RO2**2-BP**2)/(2.*R2*RO2))
PHIO2 = ACOS(RB2/RO2)
T2 = PI*R2/RN2
TO2 = T2/(2.*R2) + TAN(PHI)-PHI-TAN(PHIO2) + PHIO2
AAT1 = POB-TO2
AAT2 = AAT1 + PI/RN2
AAR = AAT2*RN2/RN1
AA = AAR*180./PI
AR = -ARR*180./PI
WRITE(*,345)AA,AR
345  FORMAT(' APPROACH ANGLE =',F10.5/, ' RECESS ANGLE =',F10.5)
Z = AP + BP
PB = 2.*PI*RB1/RN1
CR = Z/PB
WRITE(*,350)CR
350  FORMAT(' CONTACT RATIO =',F10.5)
IF (CR.GE.2.0) GO TO 800
OB = AR + 360./RN1
OE = AA-360./RN1
WRITE (*,500)OB,OE
500  FORMAT('ONE TOOTH CONTACT FROM ',F10.5,' TO ',F10.5)
800  RETURN
END

```

**The vita has been removed from
the scanned document**